Spectral analysis of very hot H-deficient [WCE]-type central stars of planetary nebulae

Graziela R. Keller[1]

<u>Colaborators</u>: Luciana Bianchi[2] and Walter J. Maciel[1]

1 *IAG/Universidade de São Paulo*

2 *The Johns Hopkins University*

This presentation is organized as follows:

- Introduction
  - Central Stars of Planetary Nebulae
  - Stellar Winds
  - Evolutionary Phase
- Model Grid
  - The CMFGEN Code
  - [WC] and PG1159 Grid
- Spectral Analysis
  - NGC 6905, NGC 5189, NGC 2867, Pb 6, and Sand 3

Introduction

◦ Central Stars of Planetary Nebulae

- **They are Hot** – T_* between 20 – 200 kK
- **Low Mass** – M_* around 0.6 $M_\odot$
- **Surrounded by a Planetary Nebula**

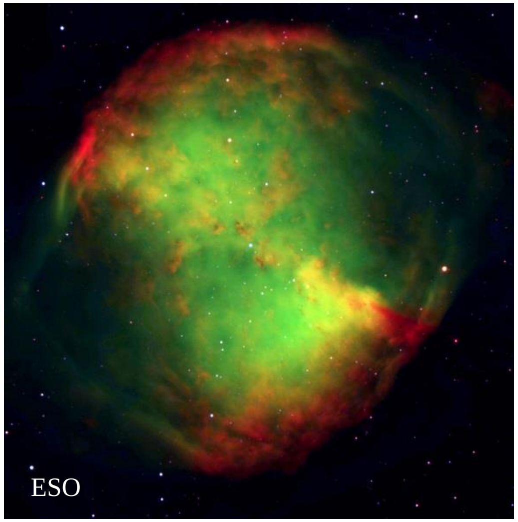

- **Present Stellar Winds** – Radiatively Driven

◦ Stellar Wind

are continuous processes

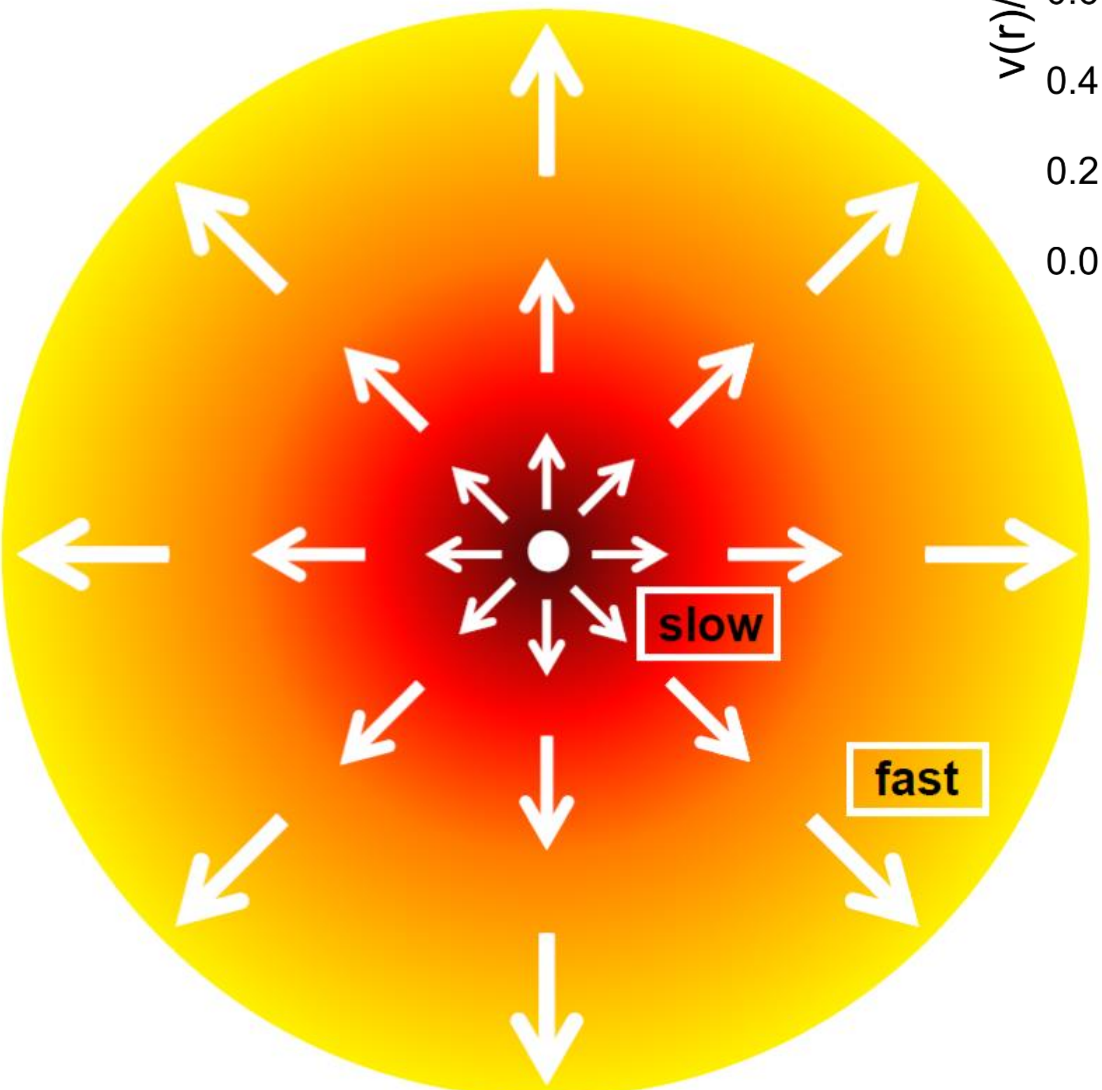

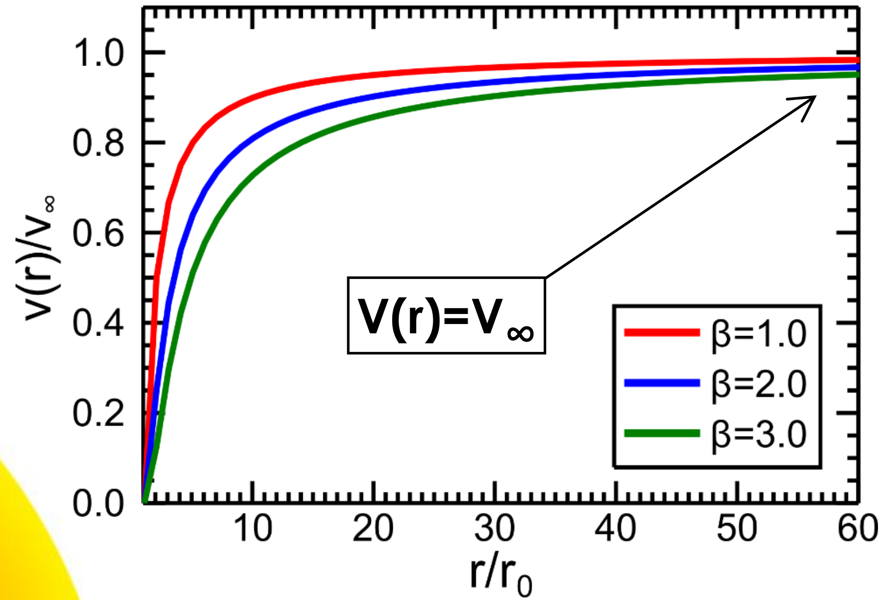

Beta velocity law:

$$v(r)=v_\infty\left(1-\frac{r_0}{r}\right)^{\beta}$$

$V_\infty \equiv$ Terminal Velocity

Mass-loss rate:

$$\dot{M}=4\pi r^2\rho(r)v(r)$$

◦ Stellar Wind

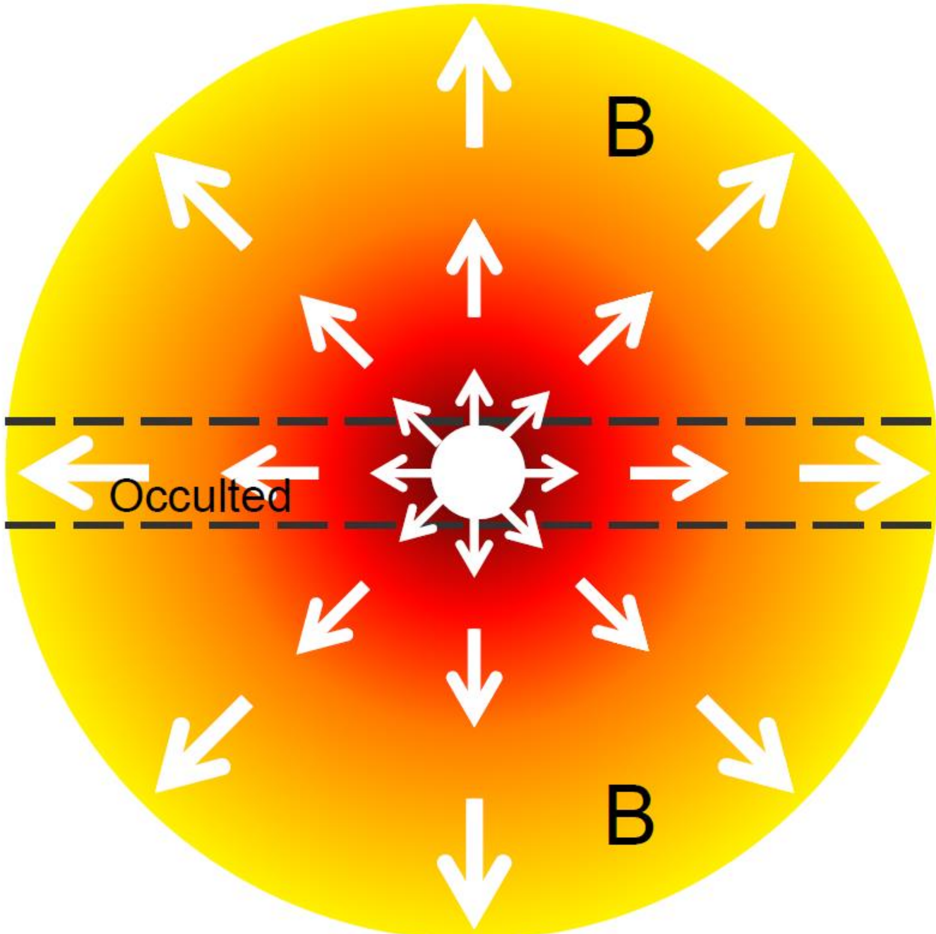

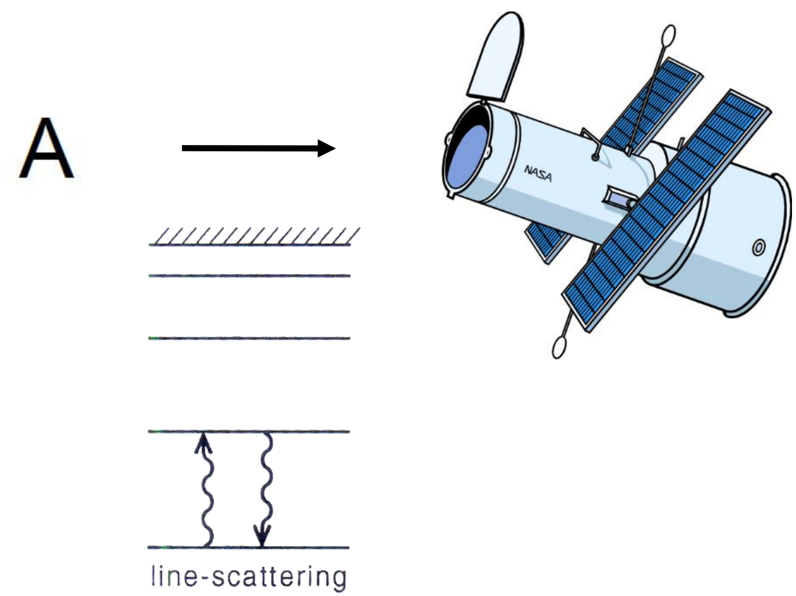

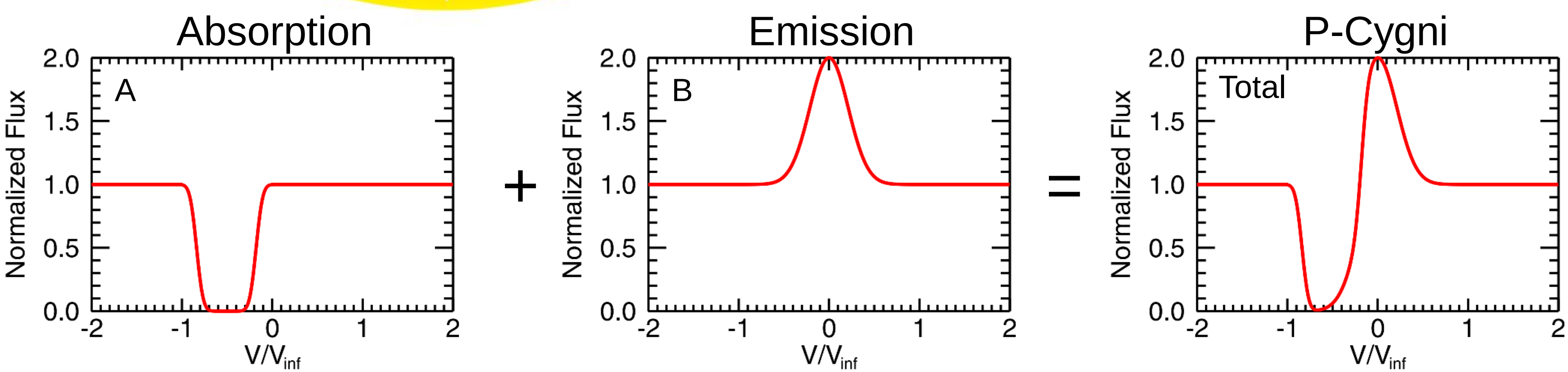

Stellar Wind

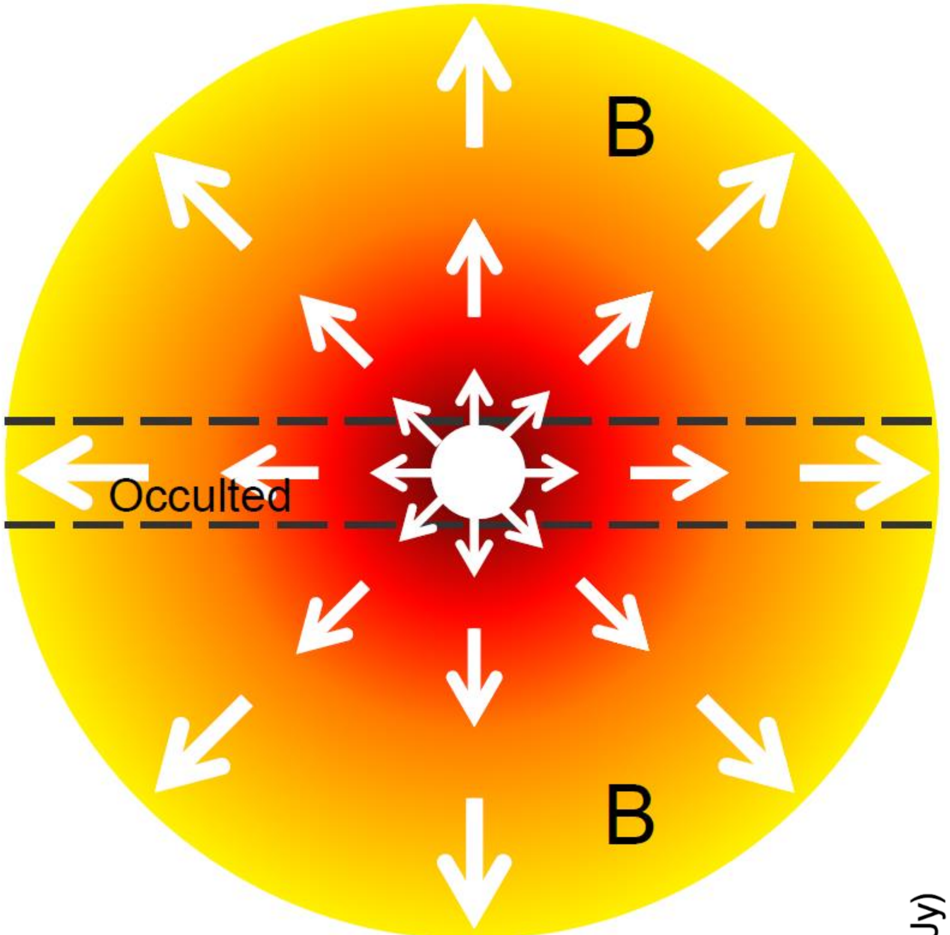

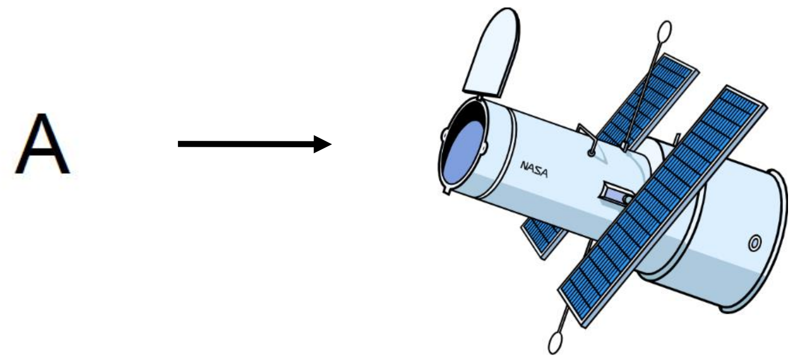

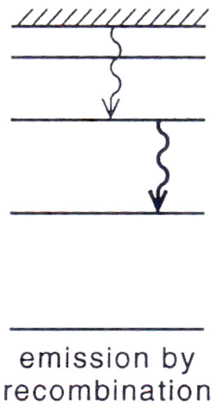

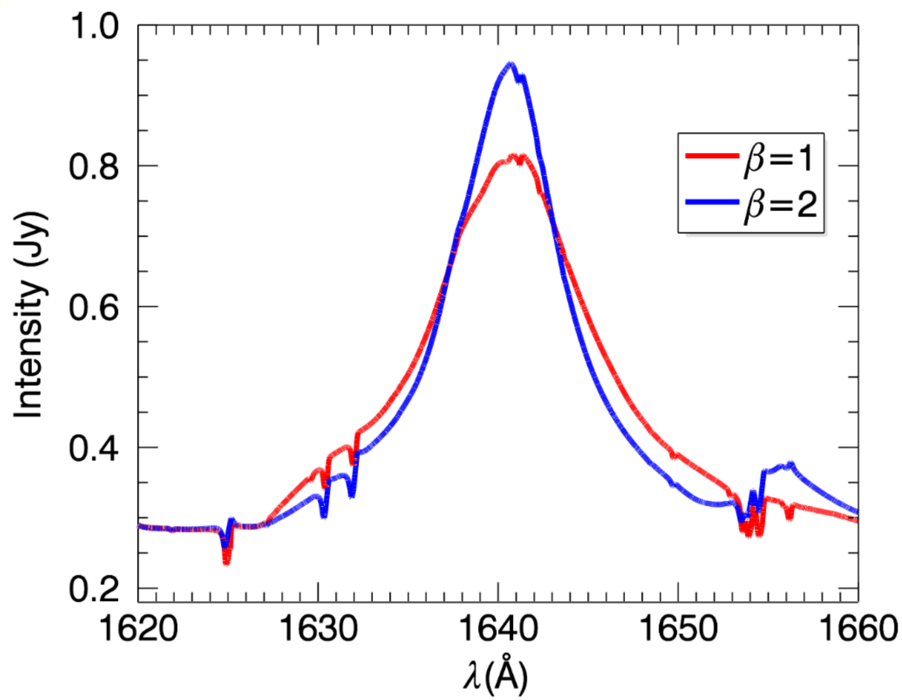

◦ Evolutionary Phase

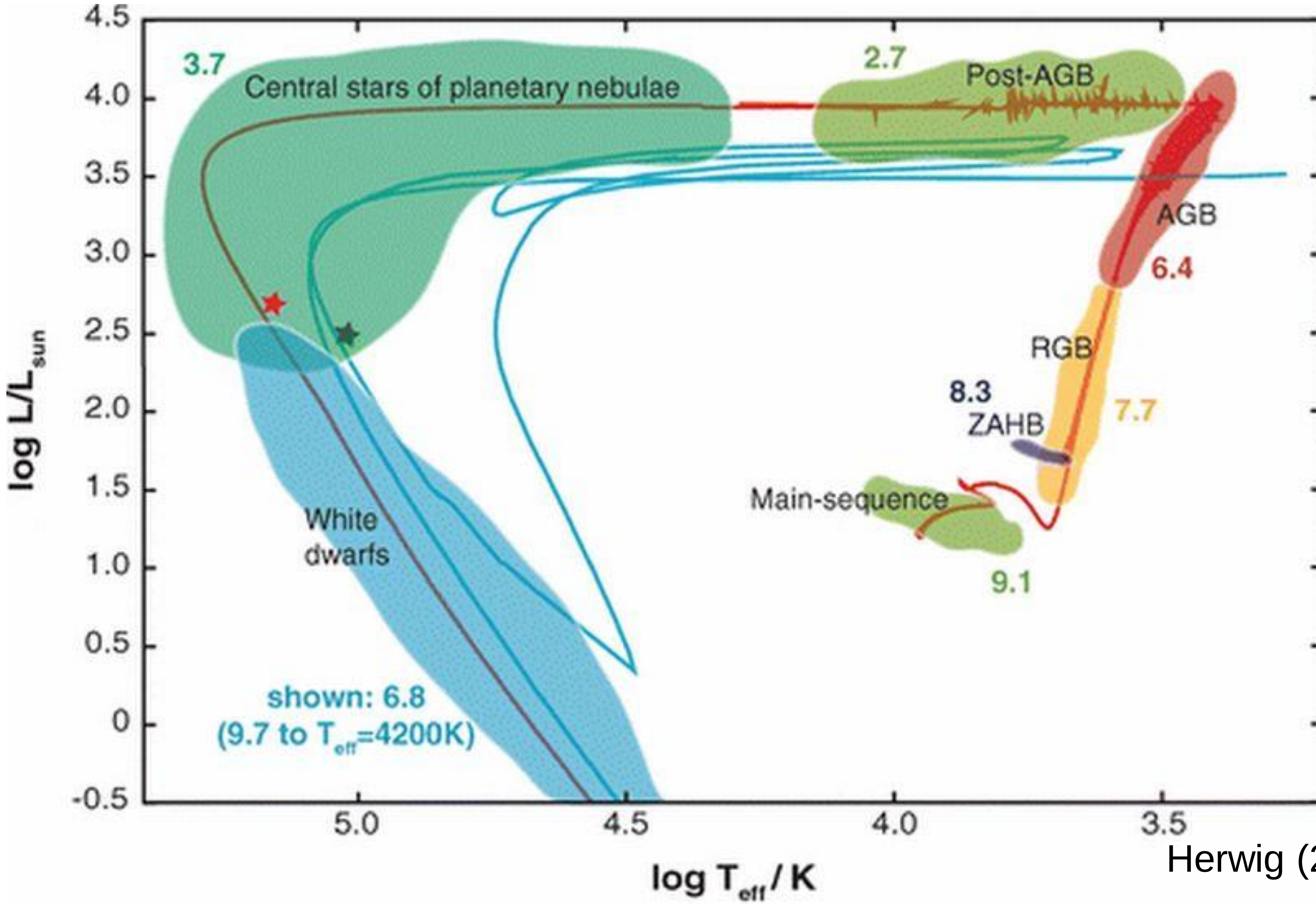

Herwig (2005)

◦ Evolutionary Phase

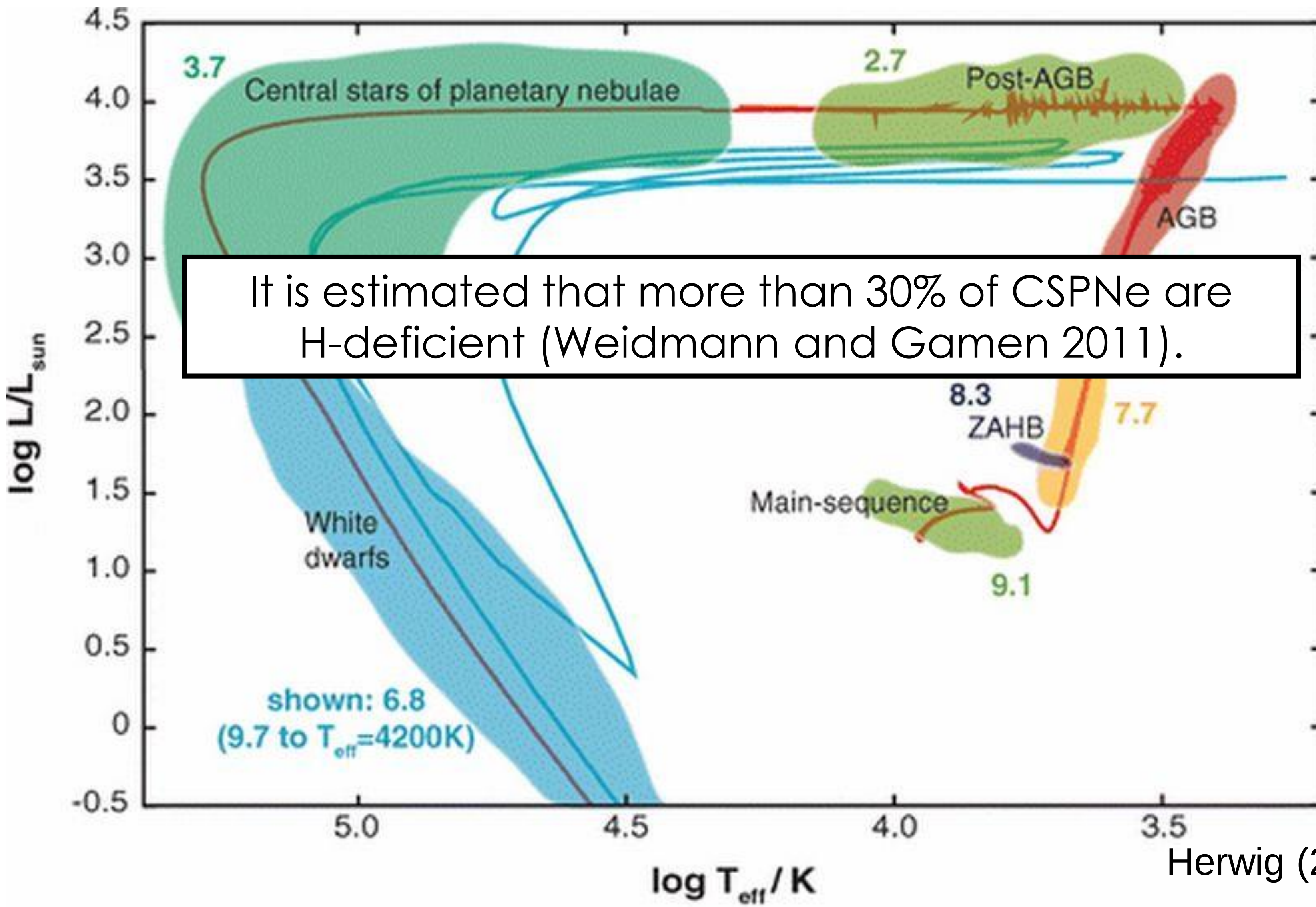

It is estimated that more than 30% of CSPNe are H-deficient (Weidmann and Gamen 2011).

Herwig (2005)

◦ Evolutionary Phase

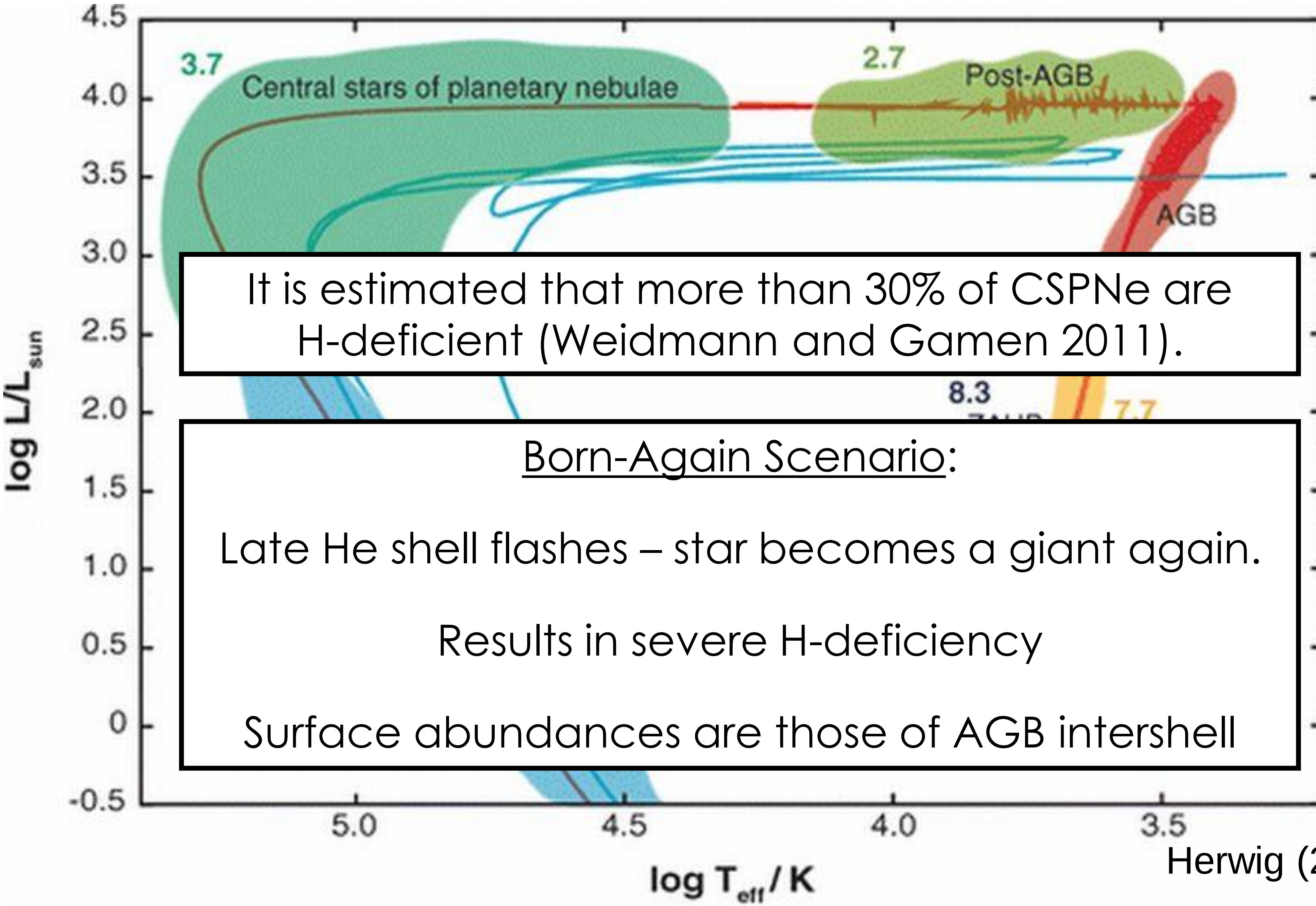

It is estimated that more than 30% of CSPNe are H-deficient (Weidmann and Gamen 2011).

<u>Born-Again Scenario</u>:

Late He shell flashes – star becomes a giant again.

Results in severe H-deficiency

Surface abundances are those of AGB intershell

Herwig (2005)

◦ Evolutionary Phase

Some famous classes of <u>H-deficient CSPNe</u> are:

[WC] – ◈ Spectra similar to massive Wolf–Rayet stars;

◈ Strong carbon and helium emission Lines;

◈ Are divided into early ([WCE]) and late type ([WCL]) objects.

PG1159 – ◈ Occupy the region at the top of the WD cooling track;

◈ Show absorption lines of highly ionized He, C, O;

◈ Show UV wind lines much weaker than the ones seen in [WC] stars;

[WC]-PG1159 – ◈ Are believed to be transition objects between the two other classes.

◦ Evolutionary Phase

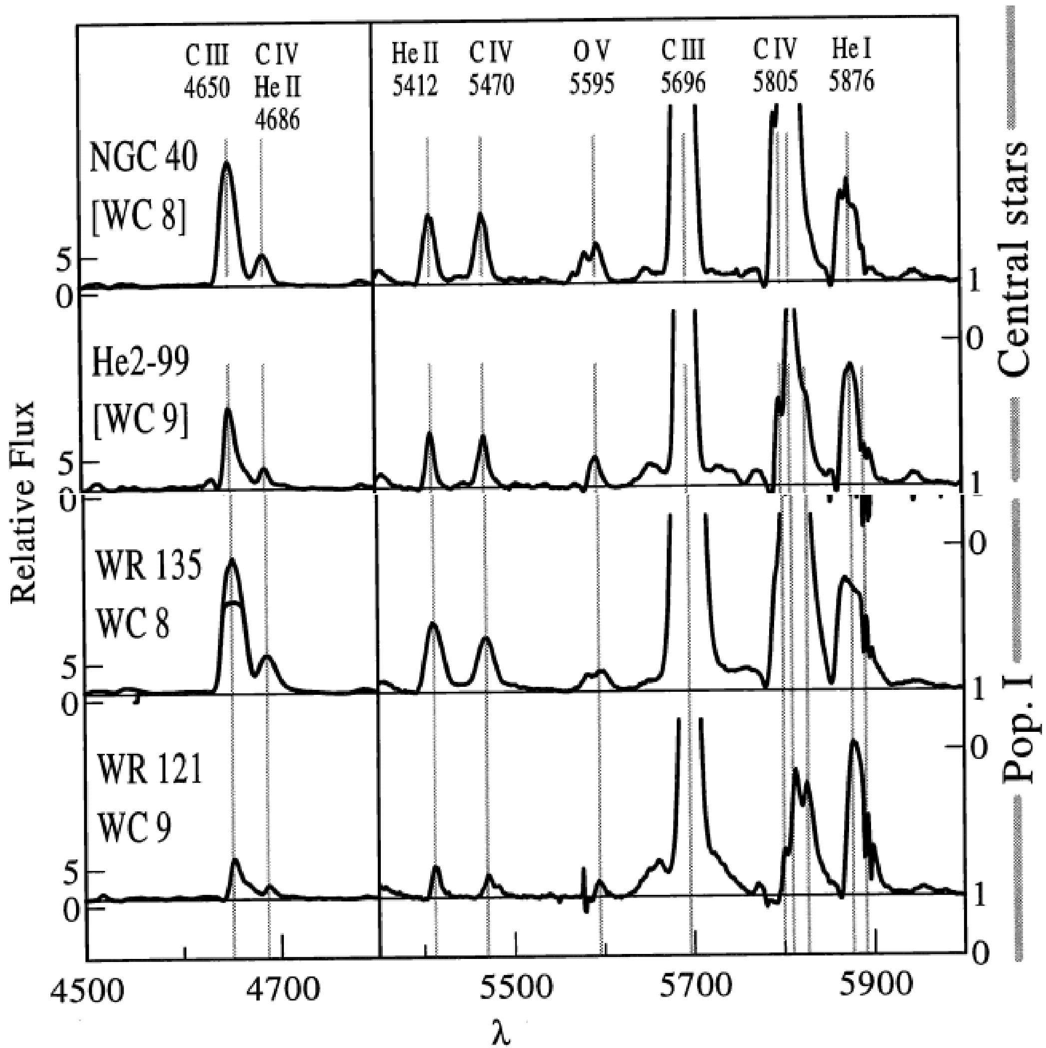

Figure 3. Comparison between Pop. I Wolf-Rayet stars and central stars with late-type WC spectra. Wavelengths in angstrom.

Hamann 1996 Ap&SS 238, 31

◦ Evolutionary Phase

[WC] X PG1159

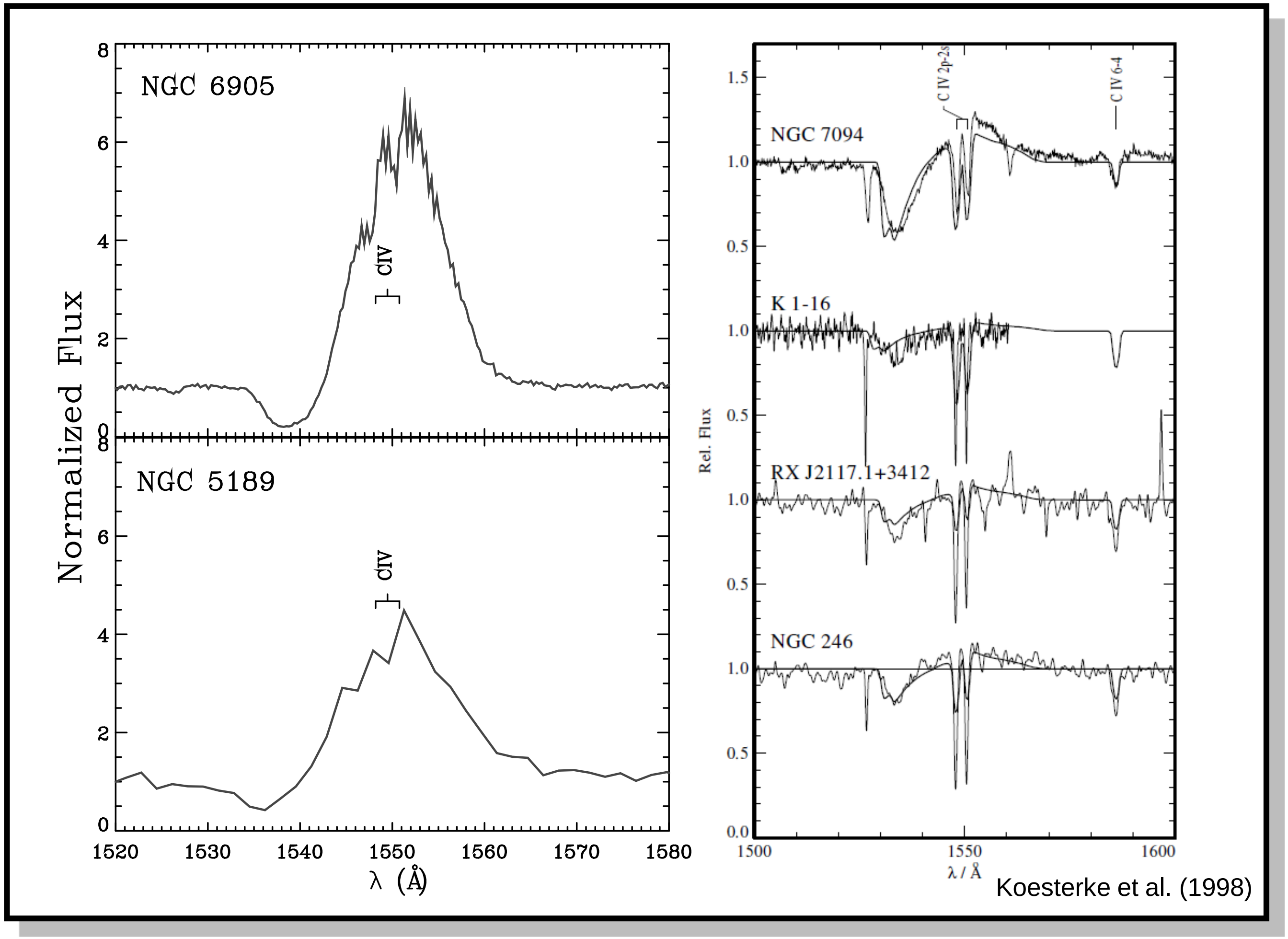

C IV λλ 1548.2, 1550.8 Å line

◦ Evolutionary Phase

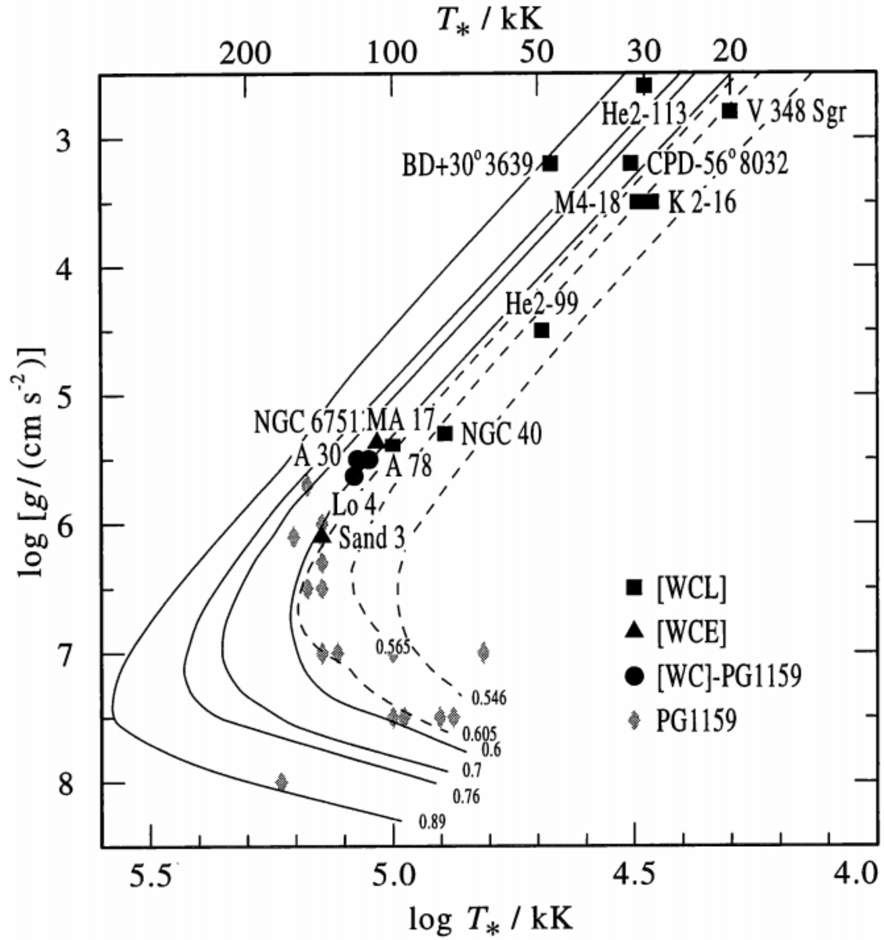

Figure 6. Central stars of Wolf-Rayet type in the lg g − lg T_*-diagram. [WCL], [WCE] and [WC]-PG 1159 subtypes are represented by squares, triangles and circles, respectively. Shaded diamonds indicate "normal" PG 1159 stars without strong mass-loss (after Dreizler *et al.* 1995). The tracks for post-AGB evolution taken from Schönberner (1983) or Wood & Faulkner (1986) (labels: mass in $M_\odot$) and are only shown for rough comparison; they are not really adequate for the considered objects, as they predict normal surface abundances.

Hamann 1996 Ap&SS 238, 31

◦ Evolutionary Phase

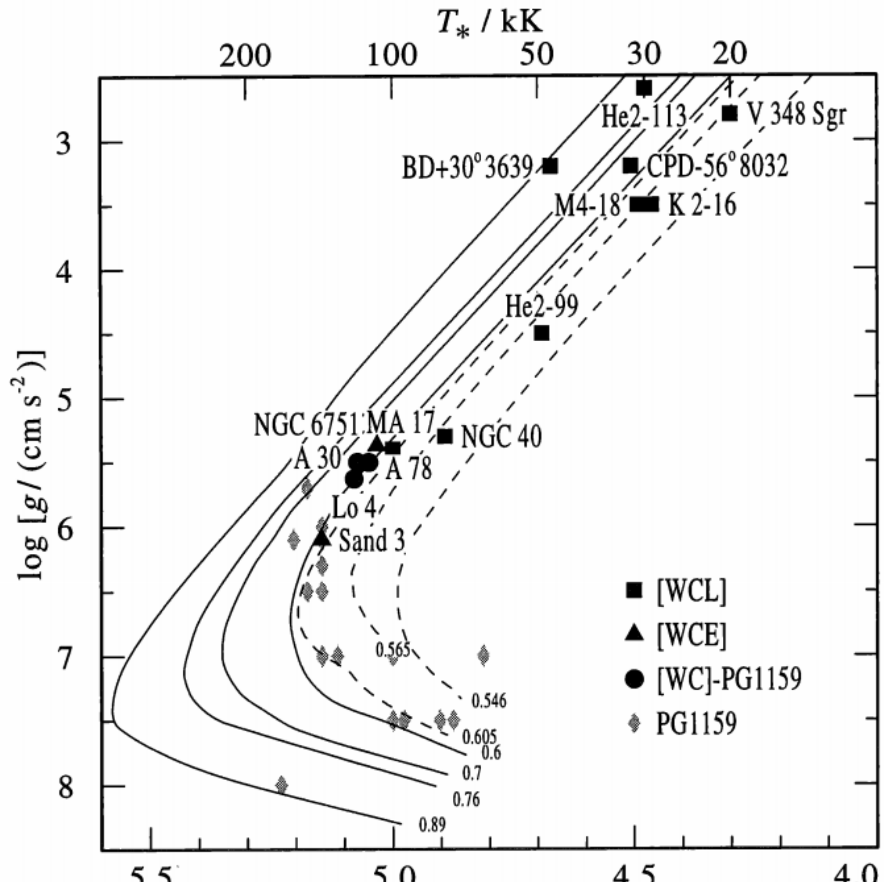

AGB → [WCL] → [WCE] → [WC]-PG1159 →PG1159 → WD

Hamann 1996 Ap&SS 238, 31

Support for this overall scenario comes from

1)Abundance patterns;
2)Proximity in evolutionary tracks;
3)post-AGB stars have been observed to re-expand and re-join the AGB, and afterwards, become a hot H-deficient CSPNe;
4)The nebulae around H-rich and [WC] and PG1159 stars are very similar and late thermal pulses happen randomly to about 20% of all post-AGB stars.

Many open questions lead to claims that the born again scenario may not be the only one forming these stars and invoking complicated close binary scenarios.

1)[WC] PN should always be too large for the position of the star on the HR diagram in comparison with a normal CS, but it is not so.
2) Recent estimates say more than 30% of CS are H-poor, while born again scenario predict at most 25%.
3)Weird abundance H-poor ejecta in objects thought to have suffered a born again scenario (oxygen-neon-magnesium Novae).
4)Frequency of the [WC] central stars in different environments;
5)Too many [WCL] central stars relative to the [WCE] and PG1159 stars.
6)Different C/He mass ratios between [WCE] and [WCL] stars

In this work, we:

Keller et al. 2011, MNRAS, 418, 705:

◈Calculated a grid of models proper to the analysis of H-poor CSPNe, covering

Far-UV, UV, optical, and IR.

◈ Made the grids available on-line at

http://dolomiti.pha.jhu.edu/planetarynebulae.html

◈Performed a differential analysis of the grid models to determine the best line diagnostics of stellar parameters.

Keller et al. 2014, MNRAS, 442, 1379:

◈Used these results to perform a uniform and systematic analysis of UV and far-UV spectra of 5 [WCE] central stars.

Model Grids

◦ CMFGEN is a state-of-the-art stellar atmosphere code which accounts for:

- Non-LTE; ✓
- Expanding atmosphere; ✓
- Line blanketing; ✓
- Wind clumping; ✓

CMFGEN

◈ **Does not** solve the dynamical equations of the wind. ✗

It requires the mass-loss rate and the velocity law to be supplied. In this work:

◈ We adopted a β-velocity law ($v(r)=v_\infty\left(1-\frac{r_0}{r}\right)^\beta$) with β=1;

◈ The mass-loss rate is a free parameter.

◦ THE GRIDS

[WC] grid → 199 models

PG1159 grid → 160 models

Models vary in L, T, logg, dM/dt, and V_∞ .

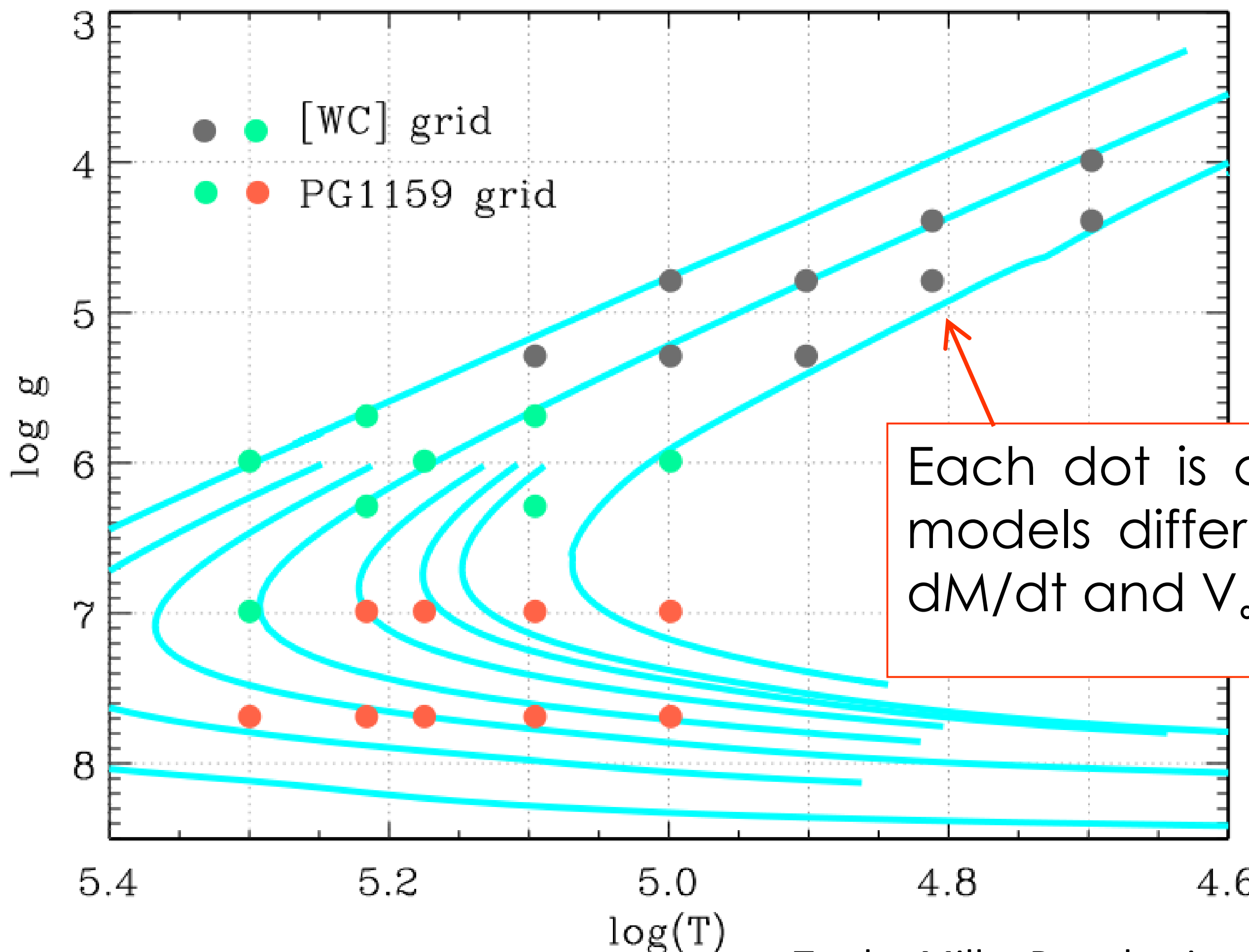

Each dot is a group of models differing only in dM/dt and V_∞.

Tracks: Miller Bertolami and Althaus (2006)

Differential Analysis of Grid Models

We performed a differential study, showing the predicted impact of parameter variation on strengths and shapes of line profiles.

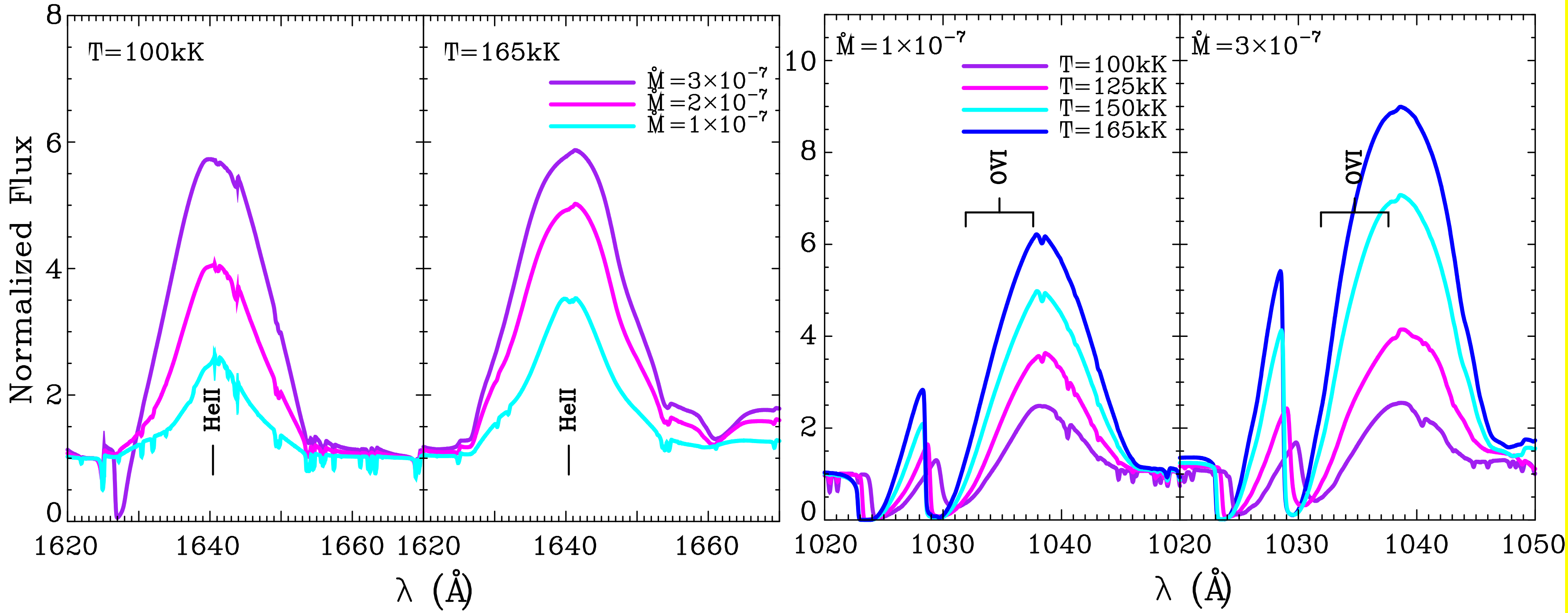

We determined the best line diagnostics of dM/dt and T_*.

Spectral Analyses

◦ Targets

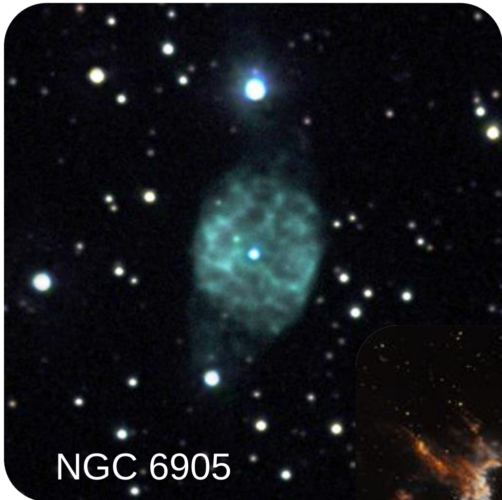

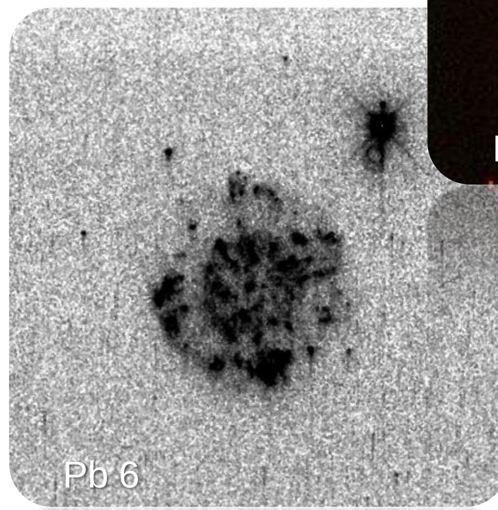

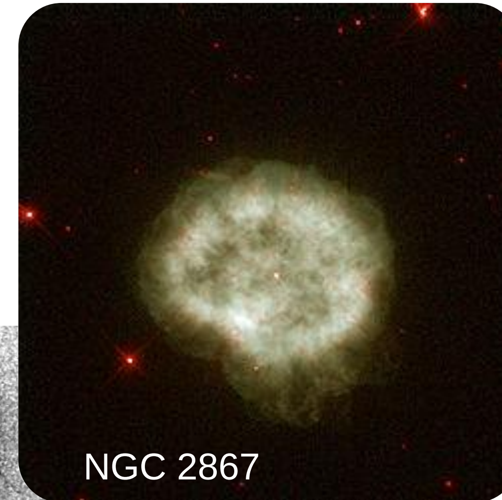

Table 1. Sample objects.

Object	v_{rad} [km s^{-1}]	Dist. [kpc]	Nebular Diam. [arcsec]	v_{exp} [km s^{-1}]	Shape
NGC 6905	-8.4[a]	1.73[e]; 1.75[f]; 1.80[g]	43.3 × 35.6[d]	43.5[a]	Elliptical
NGC 5189	-9.2[a]	0.54[e]; 0.55[f]; 0.70[g]	163.4 × 108.2[d]	36.0[a]	Quadrupolar
Pb 6	56.0[b]	4.38[e]; 4.42[f]; 4.00[g]	5.5[e]	?	Unclassified
NGC 2867	14.4[b]	1.84[e]; 2.23[f]; 1.60[g]	14.4 × 13.9[d]	18.9[a]	Elliptical
Sand 3	-92.5[c]	?	–	–	No detectable nebulosity

[a] Acker et al. (1992); [b] Peña et al. (2013); [c] Feibelman (1996b); [d] Tylenda et al. (2003); [e] Cahn et al. (1992); [f] Stanghellini et al. (2008); [g] Maciel (1984).

Image credits: NGC 6905: Bill Gillispie/Adam Block/NOAO/AURA/NSF; NGC 5189: NASA, ESA and the Hubble Heritage Team (STScI/AURA); Pb 6: MAST preview; NGC 2867: Howard Bond (STScI) and NASA/ESA.

◦ Targets: FUSE range

Far Ultraviolet Spectroscopic Explorer – (905 – 1187 Å) – resol. ~0.06 Å

Observed | Synthetic

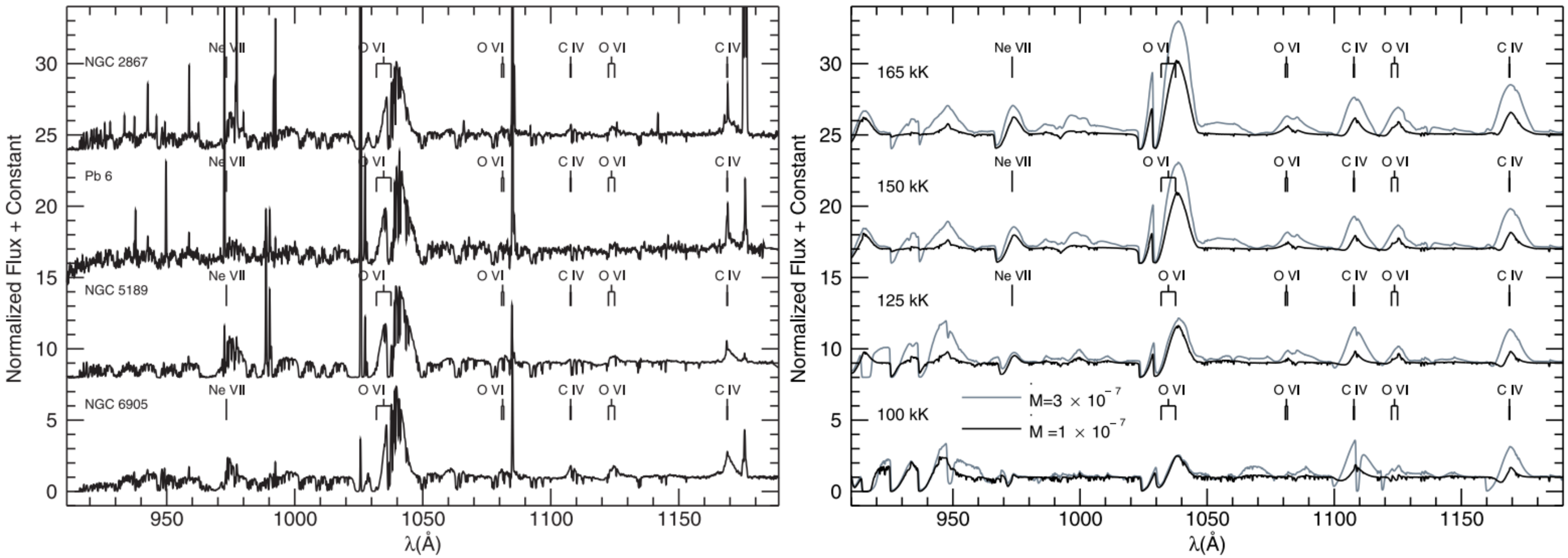

Figure 1. Left panel: FUSE spectra of the [WCE] CSPNe NGC 6905, NGC 5189, Pb 6 and NGC 2867. The numerous narrow absorptions are due to interstellar H_2, which affects the blue edge of the Ne VII P-Cygni profile. Right panel: sample synthetic spectra from our model grid, calculated for different values of stellar temperature and two different mass-loss rates (in units of $M_\odot$ yr^{-1}). All models shown adopt $v_\infty = 2500$ km s^{-1} and models of the same temperature adopt the same stellar radius. The observed and synthetic spectra shown were convolved with a Gaussian of 0.2 Å FWHM for clarity.

◦ Targets: FUSE range

Far Ultraviolet Spectroscopic Explorer – (905 – 1187 Å) – resol. ~0.06 Å

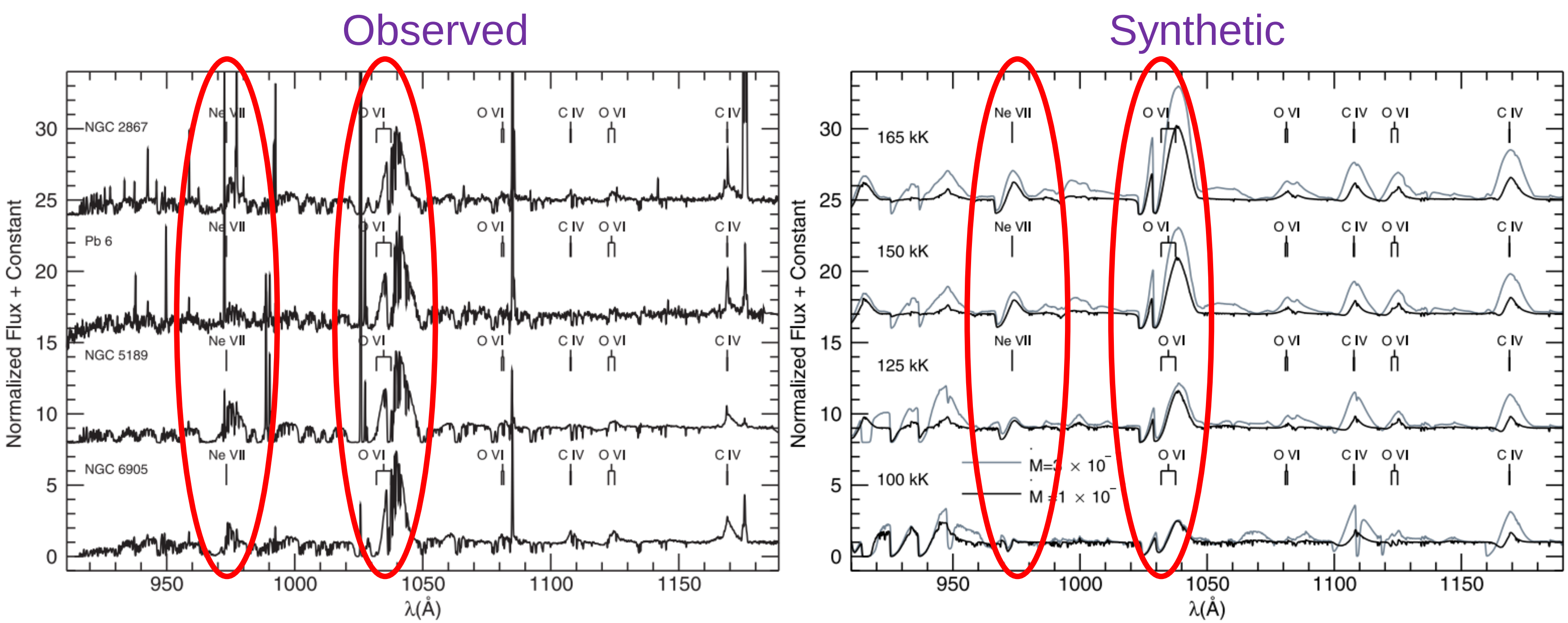

Figure 1. Left panel: FUSE spectra of the [WCE] CSPNe NGC 6905, NGC 5189, Pb 6 and NGC 2867. The numerous narrow absorptions are due to interstellar H_2, which affects the blue edge of the Ne VII P-Cygni profile. Right panel: sample synthetic spectra from our model grid, calculated for different values of stellar temperature and two different mass-loss rates (in units of $M_\odot$ yr^{-1}). All models shown adopt $v_\infty = 2500$ km s^{-1} and models of the same temperature adopt the same stellar radius. The observed and synthetic spectra shown were convolved with a Gaussian of 0.2 Å FWHM for clarity.

◦ Targets: FUSE range

Far Ultraviolet Spectroscopic Explorer – (905 – 1187 Å) – resol. ~0.06 Å

Observed Synthetic

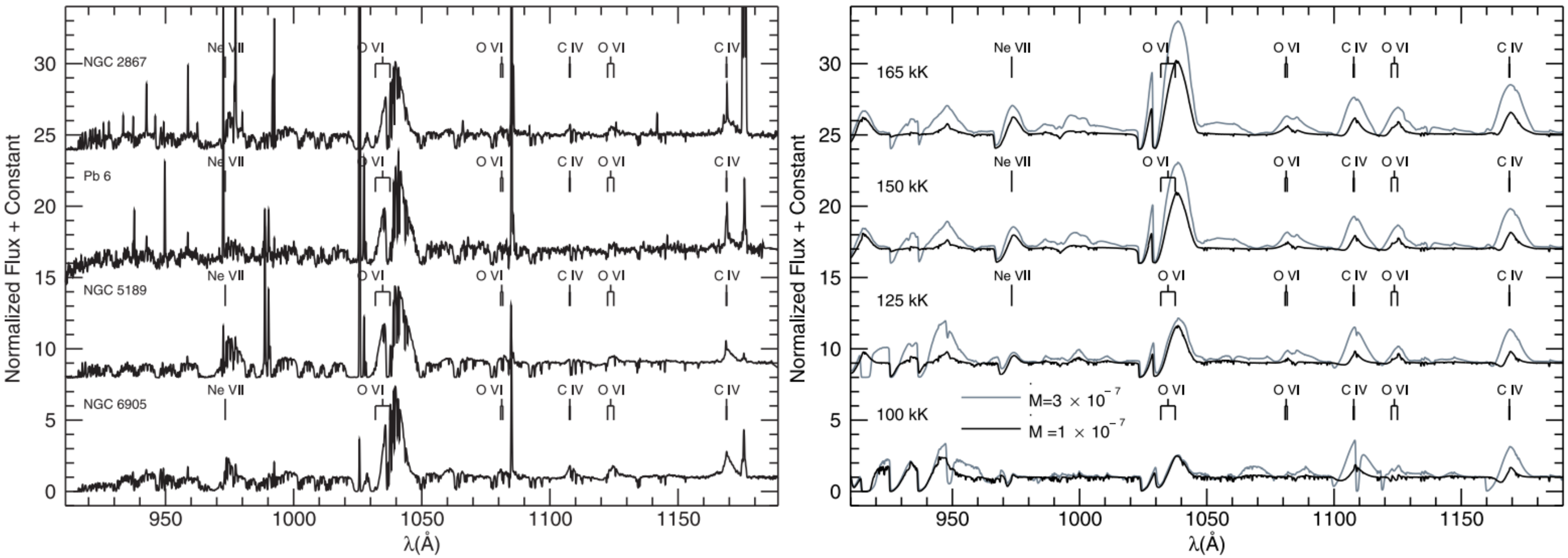

Figure 1. Left panel: FUSE spectra of the [WCE] CSPNe NGC 6905, NGC 5189, Pb 6 and NGC 2867. The numerous narrow absorptions are due to interstellar H_2, which affects the blue edge of the Ne VII P-Cygni profile. Right panel: sample synthetic spectra from our model grid, calculated for different values of stellar temperature and two different mass-loss rates (in units of $M_\odot\ yr^{-1}$). All models shown adopt $v_\infty = 2500\ km\ s^{-1}$ and models of the same temperature adopt the same stellar radius. The observed and synthetic spectra shown were convolved with a Gaussian of 0.2 Å FWHM for clarity.

◦Targets: STIS and IUE range

1200 – 1730 Å: HST/STIS – 1.2 Å ; IUE – 6.0 Å

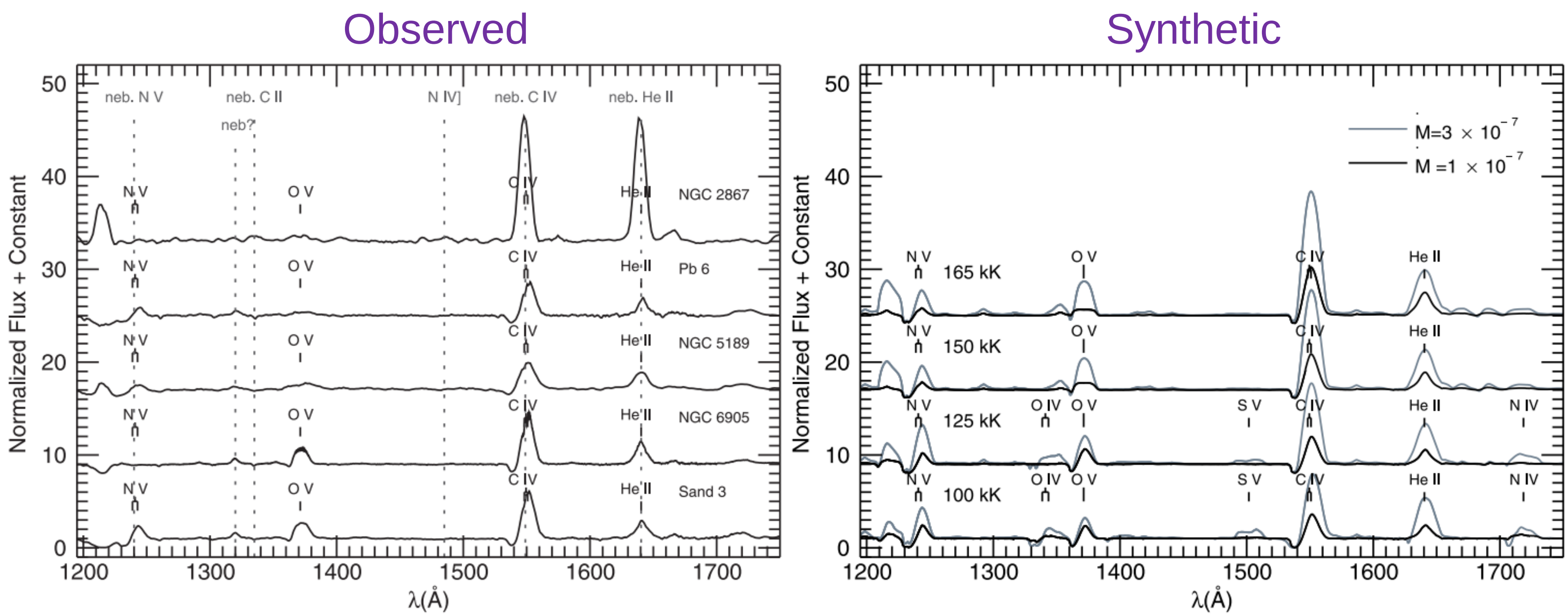

Figure 2. Left panel: HST/STIS G140L spectra of the [WCE] CSPNe NGC 6905, Pb 6 and Sand 3, and low resolution IUE spectra of NGC 5189 and NGC 2867. The dotted vertical lines indicate the location of emission lines commonly seen in PNe. Feibelman (1996b) identified the structure around 1320 Å as being a nebular [Mg V] line in the spectra of Sand 3. We, however, find evidence of its stellar origin, as we discuss on Section 2. Right panel: sample synthetic spectra from our model grid (same models as in Fig. 1), between 1200 and 1750 Å, calculated for different values of stellar temperature and two different mass-loss rates (in units of $M_\odot$ yr^{-1}). The synthetic spectra shown were convolved with a HST/STIS G140L instrumental LSF.

◦Targets: STIS and IUE range

1200 – 1730 Å: HST/STIS – 1.2 Å ; IUE – 6.0 Å

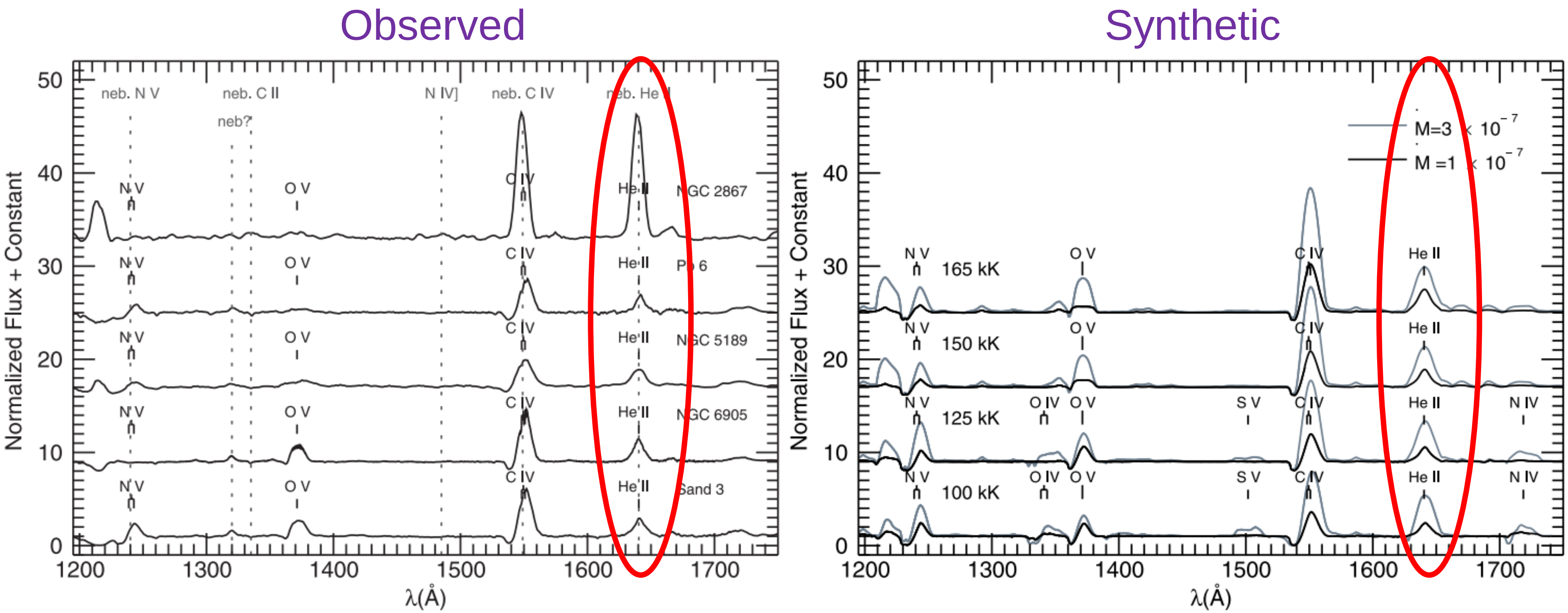

Figure 2. Left panel: HST/STIS G140L spectra of the [WCE] CSPNe NGC 6905, Pb 6 and Sand 3, and low resolution IUE spectra of NGC 5189 and NGC 2867. The dotted vertical lines indicate the location of emission lines commonly seen in PNe. Feibelman (1996b) identified the structure around 1320 Å as being a nebular [Mg V] line in the spectra of Sand 3. We, however, find evidence of its stellar origin, as we discuss on Section 2. Right panel: sample synthetic spectra from our model grid (same models as in Fig. 1), between 1200 and 1750 Å, calculated for different values of stellar temperature and two different mass-loss rates (in units of $M_\odot$ yr^{-1}). The synthetic spectra shown were convolved with a HST/STIS G140L instrumental LSF.

◦Targets: STIS and IUE range

1200 – 1730 Å: HST/STIS – 1.2 Å ; IUE – 6.0 Å

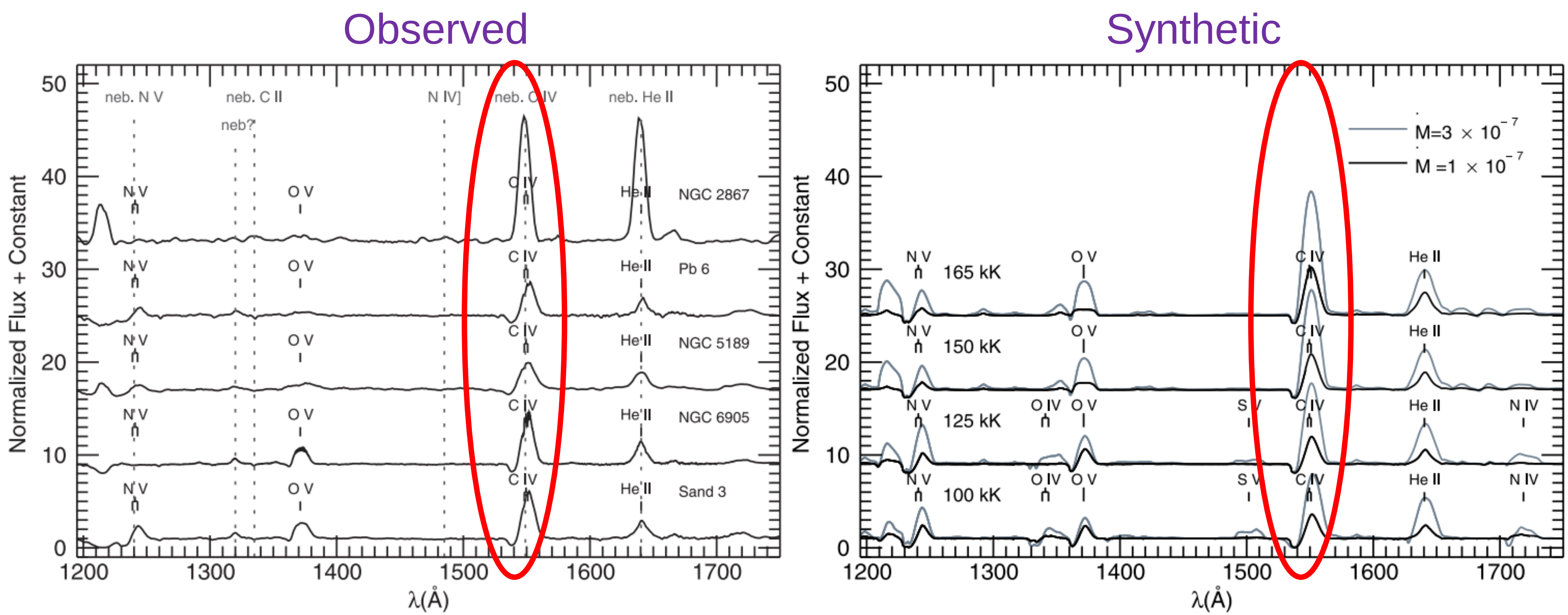

Figure 2. Left panel: HST/STIS G140L spectra of the [WCE] CSPNe NGC 6905, Pb 6 and Sand 3, and low resolution IUE spectra of NGC 5189 and NGC 2867. The dotted vertical lines indicate the location of emission lines commonly seen in PNe. Feibelman (1996b) identified the structure around 1320 Å as being a nebular [Mg V] line in the spectra of Sand 3. We, however, find evidence of its stellar origin, as we discuss on Section 2. Right panel: sample synthetic spectra from our model grid (same models as in Fig. 1), between 1200 and 1750 Å, calculated for different values of stellar temperature and two different mass-loss rates (in units of $M_\odot$ yr^{-1}). The synthetic spectra shown were convolved with a HST/STIS G140L instrumental LSF.

◦Targets: STIS and IUE range

1200 – 1730 Å: HST/STIS – 1.2 Å ; IUE – 6.0 Å

Observed

Synthetic

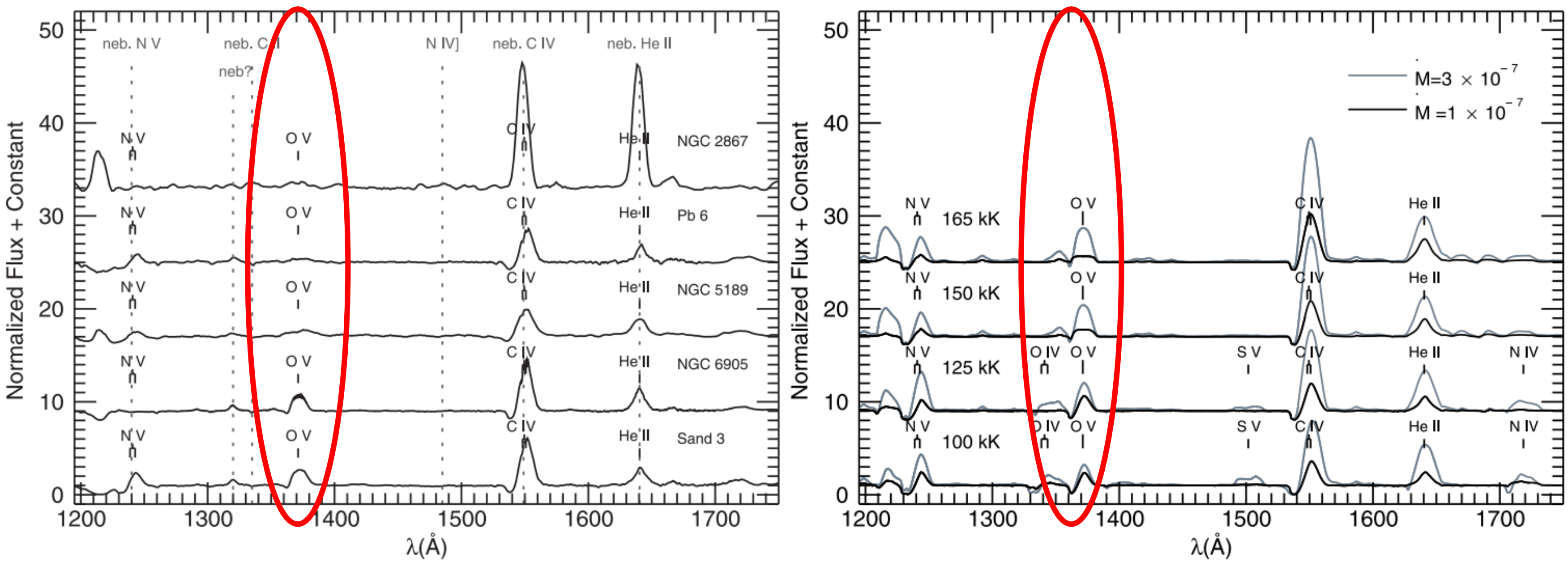

Figure 2. Left panel: HST/STIS G140L spectra of the [WCE] CSPNe NGC 6905, Pb 6 and Sand 3, and low resolution IUE spectra of NGC 5189 and NGC 2867. The dotted vertical lines indicate the location of emission lines commonly seen in PNe. Feibelman (1996b) identified the structure around 1320 Å as being a nebular [Mg V] line in the spectra of Sand 3. We, however, find evidence of its stellar origin, as we discuss on Section 2. Right panel: sample synthetic spectra from our model grid (same models as in Fig. 1), between 1200 and 1750 Å, calculated for different values of stellar temperature and two different mass-loss rates (in units of $M_{\odot}$ yr^{-1}). The synthetic spectra shown were convolved with a HST/STIS G140L instrumental LSF.

◦Targets: STIS and IUE range

1200 – 1730 Å: HST/STIS – 1.2 Å ; IUE – 6.0 Å

Observed

Synthetic

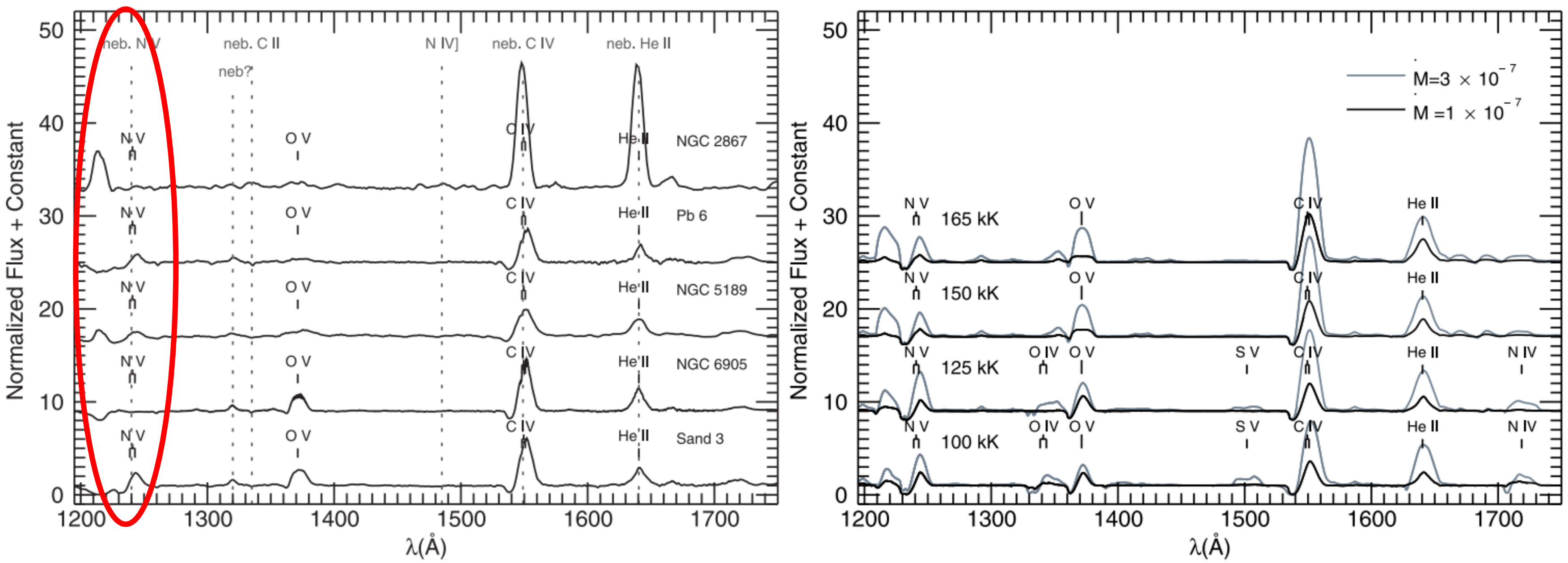

Figure 2. Left panel: HST/STIS G140L spectra of the [WCE] CSPNe NGC 6905, Pb 6 and Sand 3, and low resolution IUE spectra of NGC 5189 and NGC 2867. The dotted vertical lines indicate the location of emission lines commonly seen in PNe. Feibelman (1996b) identified the structure around 1320 Å as being a nebular [Mg V] line in the spectra of Sand 3. We, however, find evidence of its stellar origin, as we discuss on Section 2. Right panel: sample synthetic spectra from our model grid (same models as in Fig. 1), between 1200 and 1750 Å, calculated for different values of stellar temperature and two different mass-loss rates (in units of $M_{\odot}\ yr^{-1}$). The synthetic spectra shown were convolved with a HST/STIS G140L instrumental LSF.

◦Targets: STIS and IUE range

1200 – 1730 Å: HST/STIS – 1.2 Å ; IUE – 6.0 Å

Observed   Synthetic

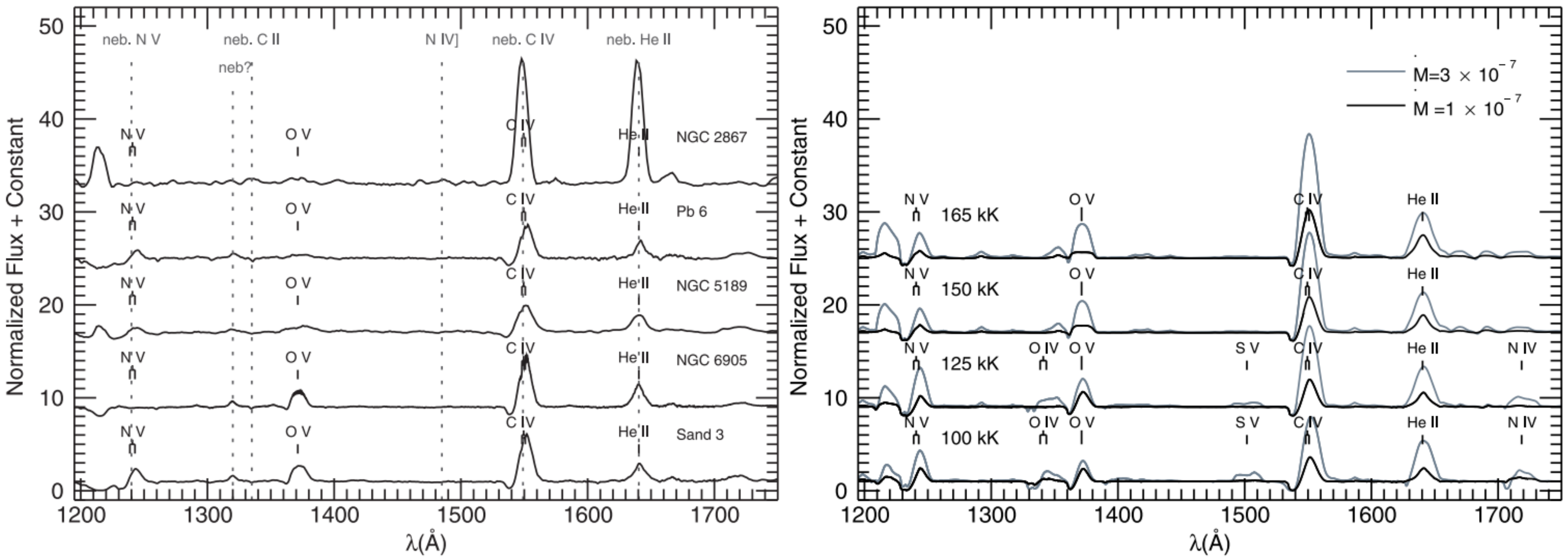

Figure 2. Left panel: HST/STIS G140L spectra of the [WCE] CSPNe NGC 6905, Pb 6 and Sand 3, and low resolution IUE spectra of NGC 5189 and NGC 2867. The dotted vertical lines indicate the location of emission lines commonly seen in PNe. Feibelman (1996b) identified the structure around 1320 Å as being a nebular [Mg V] line in the spectra of Sand 3. We, however, find evidence of its stellar origin, as we discuss on Section 2. Right panel: sample synthetic spectra from our model grid (same models as in Fig. 1), between 1200 and 1750 Å, calculated for different values of stellar temperature and two different mass-loss rates (in units of $M_\odot$ yr^{-1}). The synthetic spectra shown were convolved with a HST/STIS G140L instrumental LSF.

Additional Ions

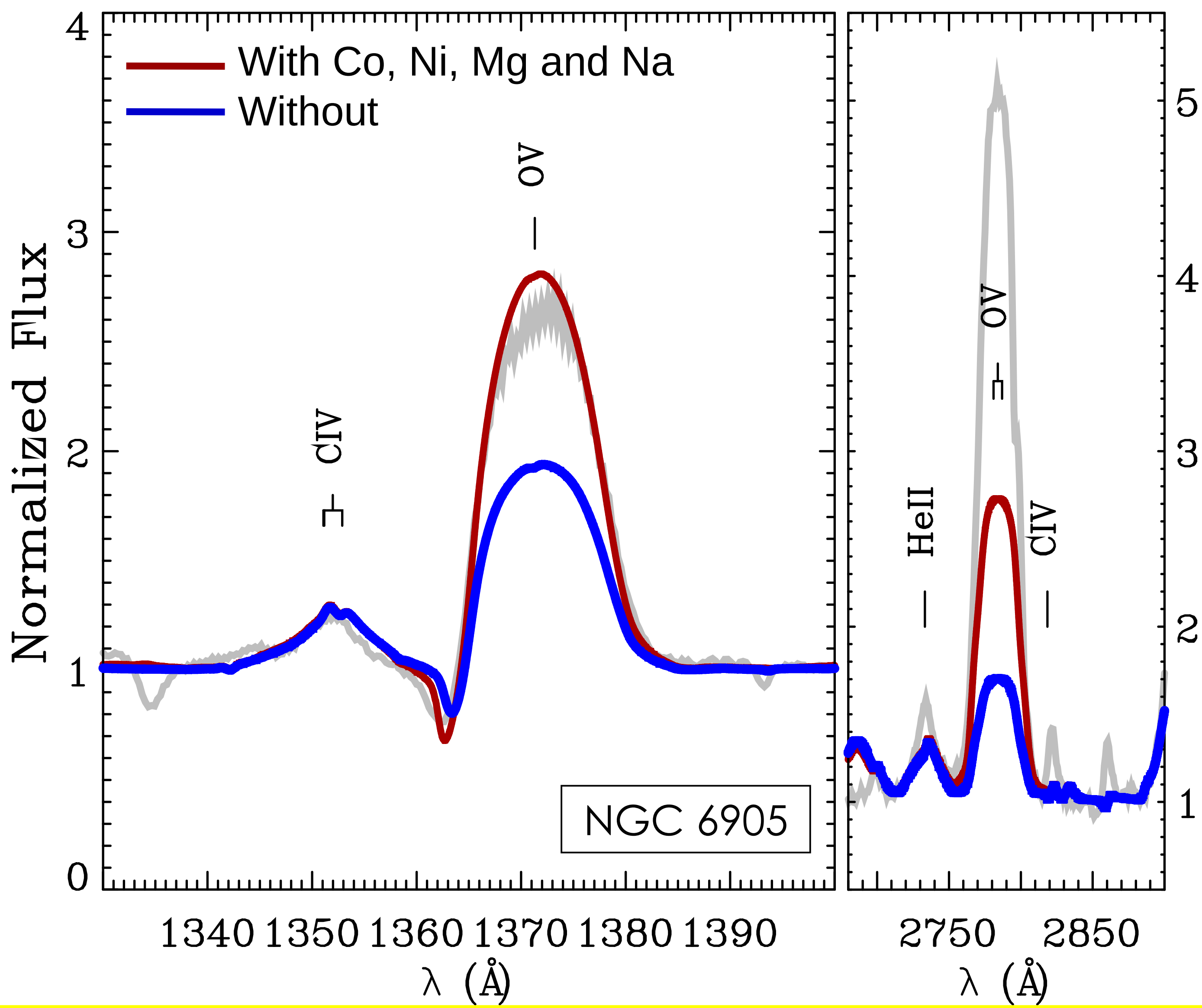

Best Fit Models

Far-UV
FUSE spectra

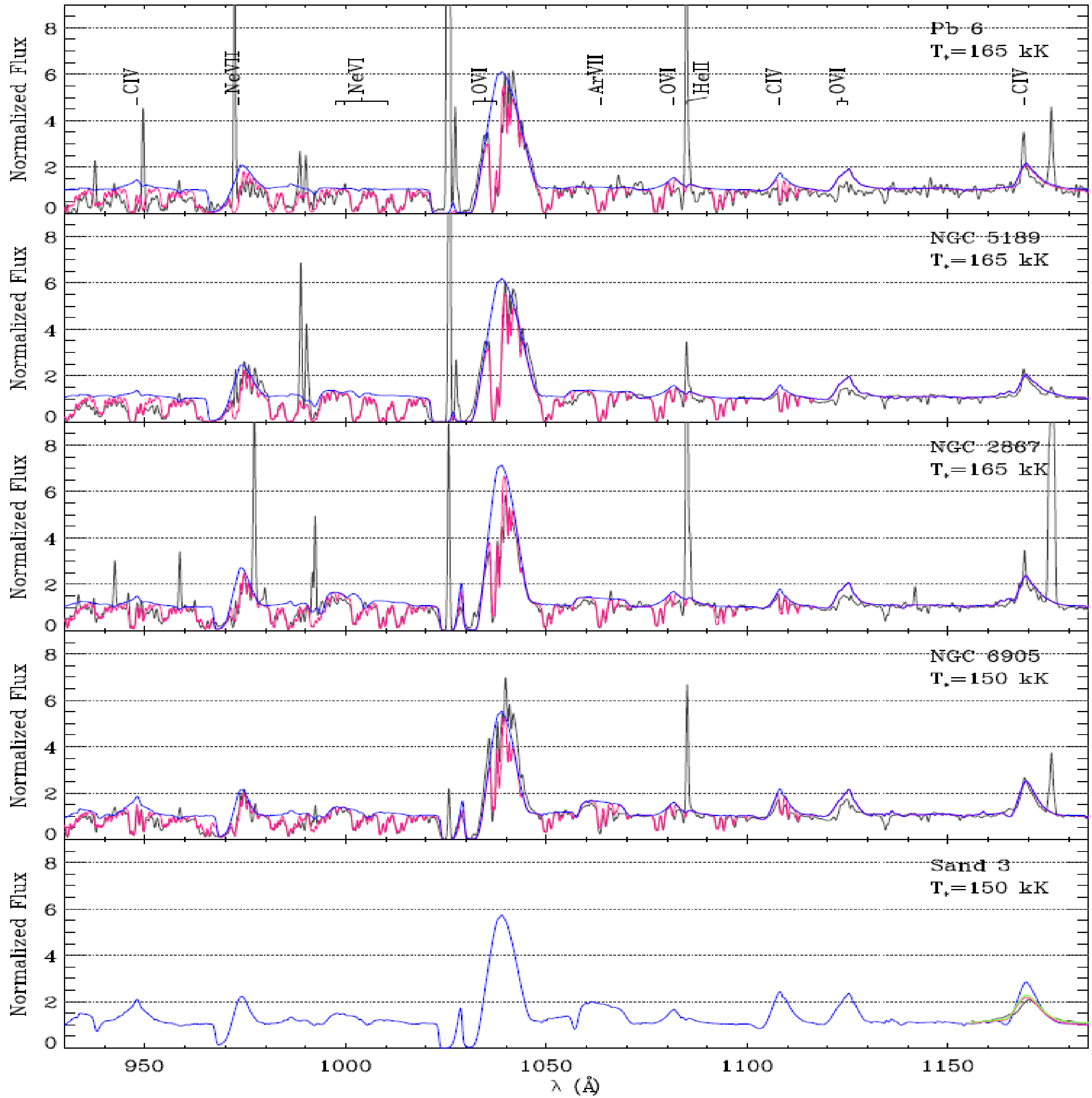

Best Fit Models

(IUE and HST/STIS spectra)

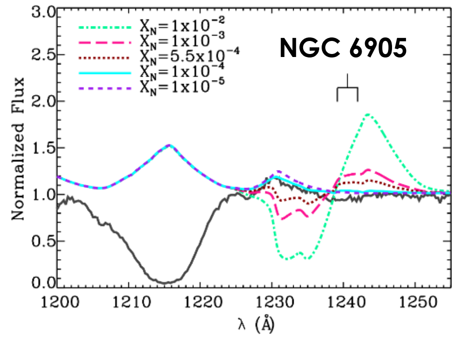

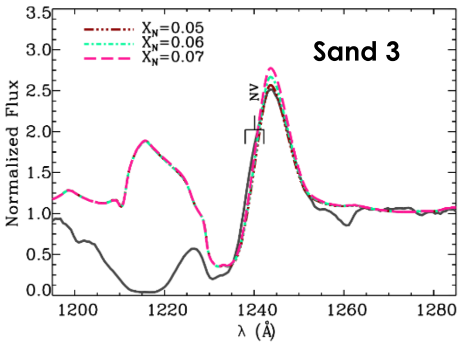

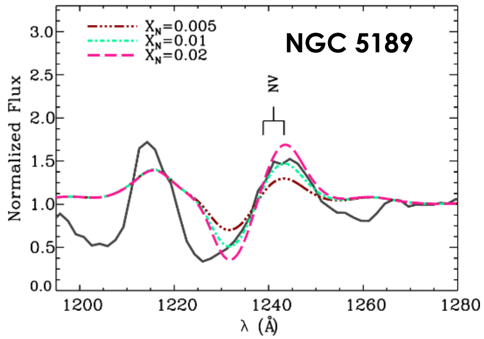

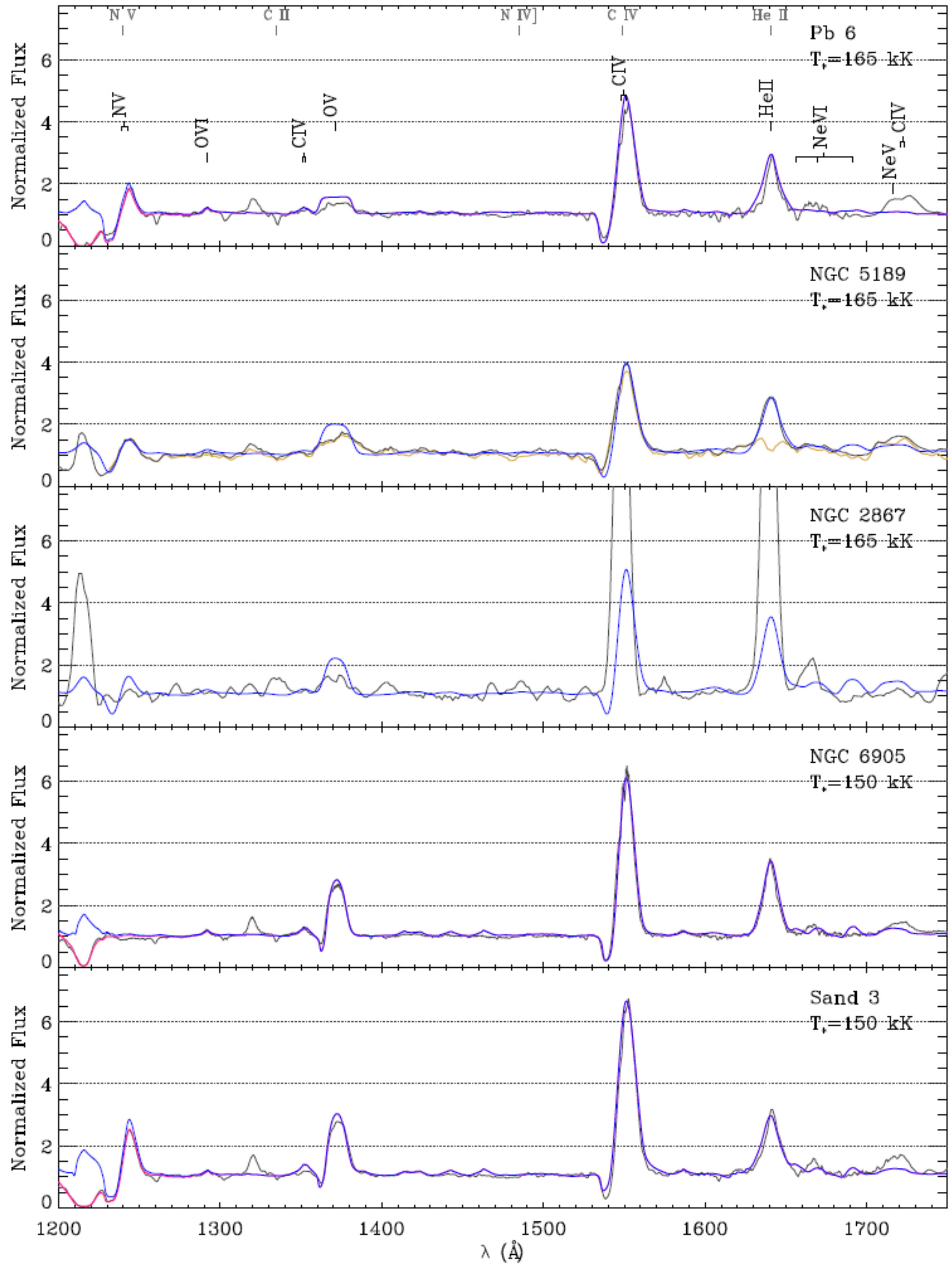

Interstellar Lyman-α

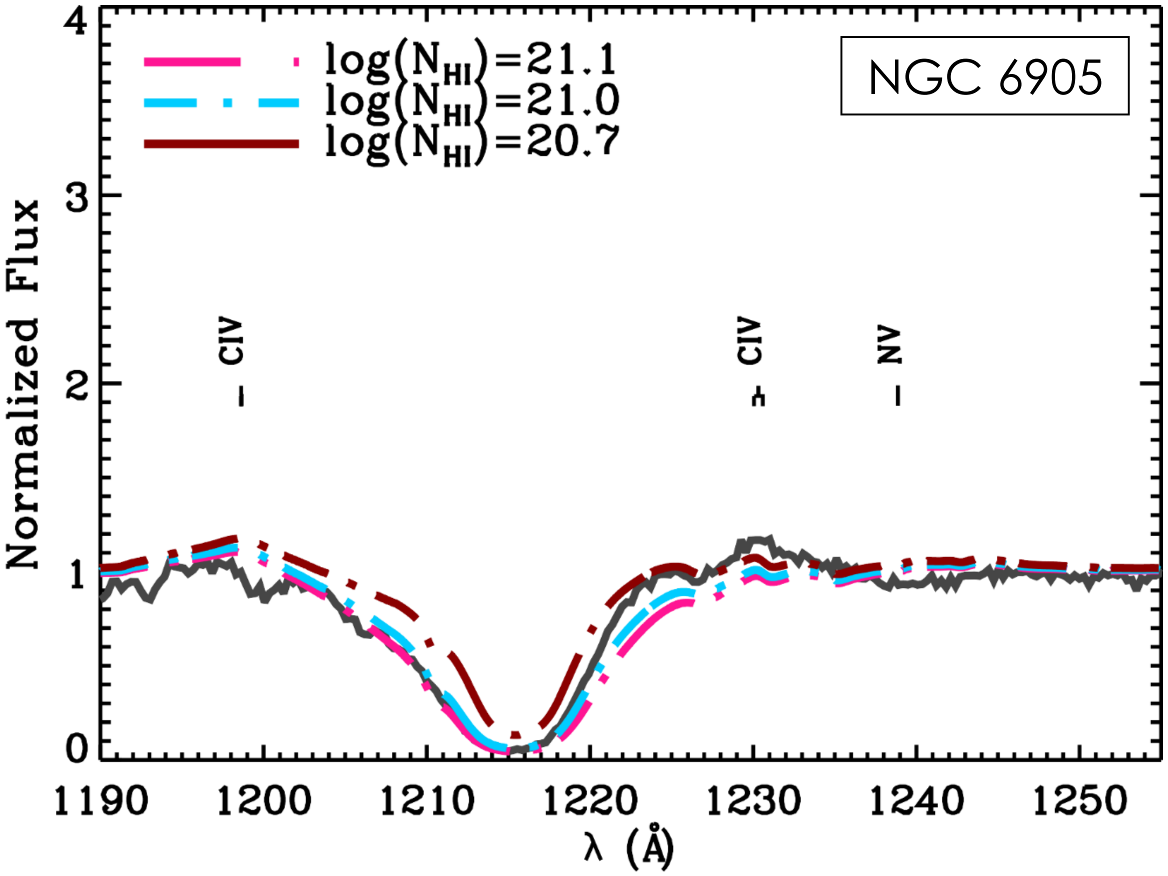

Results

Table 5. Parameters of our best-fitting models for the sample objects and distance dependent parameters. X_{He}, X_C, X_N, X_O, and X_{Ne} are the helium, carbon, nitrogen, oxygen, and neon mass fractions, respectively. For the discussion on the derived parameters and errors, see text. Results by other authors are also shown.

Object	Pb 6		NGC 6905			NGC 5189		Sand 3			NGC 2867	
	t.w.	KH1997a	t.w.	M2007	KH1997a	t.w.	KH1997a	t.w.	KH1997b	BH1982	t.w.	KH1997a
T_* [kK]	165	140	150	149.6	141	165	135	150	140	200	165	141
R_t [$R_\odot$]	9.9	4.5	10.7	10.5	3.4	9.9	5.0	9.4	3.0		8.5	4.0
v_∞ [km/s]	2500	3000	2000	1890	1800	2500	3000	2200	2200	2700	2000	1800
X_{He}	0.49	0.617	0.45	0.49	0.60	0.58	0.757	0.28	0.615	0.38	0.60	0.66
X_C	0.35	0.24	0.45	0.40	0.25	0.25	0.16	0.55	0.26	0.54	0.25	0.25
X_O	0.12	0.14	0.08	0.10	0.15	0.12	0.08	0.08	0.12	0.08	0.10	0.09
X_N	0.03	0.003	0.00011	$<$0.001	0	0.01	0.003	0.07	0.005		0.01[b]	0
X_{Ne}	0.01		0.02			0.04		0.02[b]			0.04	
ξ_{max} [km/s]	200		150			200		150			200	
d[c] [kpc]	4.38		1.70			0.55		0.80[a]			1.84	
distance dependent parameters												
R_* [$R_\odot$]	0.06		0.09			0.03		0.12[a]			0.05	
$\log L/L_\odot$	3.43		3.56			2.73		3.84[a]			3.15	
$\log \dot{M}$ [$M_\odot\,yr^{-1}$]	-7.29		-7.21			-7.81		-6.89[a]			-7.50	

t.w.=this work; KH1997a=Koesterke and Hamann (1997a); KH1997b=Koesterke and Hamann (1997b); M2007=Marcolino et al. (2007b), BH1982=Barlow and Hummer (1982)

[a] Values obtained assuming $\log L/L_\odot$=3.84.

[b] Not constrained. Value assumed on the grid models was kept.

[c] Distances from Table 1.

Ions

Table 3. Ion superlevels and levels of the best-fitting final models for the central stars of NGC 6905, Sand 3, Pb 6, NGC 2867, and NGC 5189.

Element	I	II	III	IV	V	VI	VII	VIII	IX	X	XI
He	40,45	22,30	1								
C				49,64	1						
N					13,21	1					
O				29,48[a]	58,163	41,47	1				
Ne				45,355[a]	37,166	36,202	38,182	24,47	1		
Na						52,452	37,251	72,214	27,71	1	
Mg					43,311	46,444	54,476	1			
Si				22,33	33,71[a]	33,98[a]	1[a]				
P					16,62	1					
S						28,58	1				
Ar						30,205	33,174	57,72	1		
Ca						47,108[a]	55,514[a]	54,445[a]	35,367[a]	31,79[a]	1[a]
Fe						44,433[a]	41,252	53,324	52,490	43,210	1
Co							45,1000	50,1217	24,355	1	
Ni							37,308	113,1000	75,1217	1	

Results

Table 5. Parameters of our best-fitting models for the sample objects and distance dependent parameters. X_{He}, X_C, X_N, X_O, and X_{Ne} are the helium, carbon, nitrogen, oxygen, and neon mass fractions, respectively. For the discussion on the derived parameters and errors, see text. Results by other authors are also shown.

Object	Pb 6		NGC 6905			NGC 5189		Sand 3			NGC 2867	
	t.w.	KH1997a	t.w.	M2007	KH1997a	t.w.	KH1997a	t.w.	KH1997b	BH1982	t.w.	KH1997a
T_* [kK]	165	140	150	149.6	141	165	135	150	140	200	165	141
R_t [$R_\odot$]	9.9	4.5	10.7	10.5	3.4	9.9	5.0	9.4	3.0		8.5	4.0
v_∞ [km/s]	2500	3000	2000	1890	1800	2500	3000	2200	2200	2700	2000	1800
X_{He}	0.49	0.617	0.45	0.49	0.60	0.58	0.757	0.28	0.615	0.38	0.60	0.66
X_C	0.35	0.24	0.45	0.40	0.25	0.25	0.16	0.55	0.26	0.54	0.25	0.25
X_O	0.12	0.14	0.08	0.10	0.15	0.12	0.08	0.08	0.12	0.08	0.10	0.09
X_N	0.03	0.003	0.00011	<0.001	0	0.01	0.003	0.07	0.005		0.01[b]	0
X_{Ne}	0.01		0.02			0.04		0.02[b]			0.04	
ξ_{max} [km/s]	200		150			200		150			200	
d[c][kpc]	4.38		1.70			0.55		0.80[a]			1.84	
distance dependent parameters												
R_* [$R_\odot$]	0.06		0.09			0.03		0.12[a]			0.05	
$\log L/L_\odot$	3.43		3.56			2.73		3.84[a]			3.15	
$\log \dot{M}$ [$M_\odot\,yr^{-1}$]	-7.29		-7.21			-7.81		-6.89[a]			-7.50	

t.w.=this work; KH1997a=Koesterke and Hamann (1997a); KH1997b=Koesterke and Hamann (1997b); M2007=Marcolino et al. (2007b), BH1982=Barlow and Hummer (1982)

[a] Values obtained assuming $\log L/L_\odot$=3.84.

[b] Not constrained. Value assumed on the grid models was kept.

[c] Distances from Table 1.

Results

Table 5. Parameters of our best-fitting models for the sample objects and distance dependent parameters. X_{He}, X_C, X_N, X_O, and X_{Ne} are the helium, carbon, nitrogen, oxygen, and neon mass fractions, respectively. For the discussion on the derived parameters and errors, see text. Results by other authors are also shown.

Object	Pb 6		NGC 6905			NGC 5189		Sand 3			NGC 2867	
	t.w.	KH1997a	t.w.	M2007	KH1997a	t.w.	KH1997a	t.w.	KH1997b	BH1982	t.w.	KH1997a
T_* [kK]	165	140	150	149.6	141	165	135	150	140	200	165	141
R_t [$R_\odot$]	9.9	4.5	10.7	10.5	3.4	9.9	5.0	9.4	3.0		8.5	4.0
v_∞ [km/s]	2500	3000	2000	1890	1800	2500	3000	2200	2200	2700	2000	1800
X_{He}	0.49	0.617	0.45	0.49	0.60	0.58	0.757	0.28	0.615	0.38	0.60	0.66
X_C	0.35	0.24	0.45	0.40	0.25	0.25	0.16	0.55	0.26	0.54	0.25	0.25
X_O	0.12	0.14	0.08	0.10	0.15	0.12	0.08	0.08	0.12	0.08	0.10	0.09
X_N	0.03	0.003	0.00011	<0.001	0	0.01	0.003	0.07	0.005		0.01[b]	0
X_{Ne}	0.01		0.02			0.04		0.02[b]			0.04	
ξ_{max} [km/s]	200		150			200		150			200	
d[c][kpc]	4.38		1.70			0.55		0.80[a]			1.84	
distance dependent parameters												
R_* [$R_\odot$]	0.06		0.09			0.03		0.12[a]			0.05	
$\log L/L_\odot$	3.43		3.56			2.73		3.84[a]			3.15	
$\log \dot{M}$ [$M_\odot yr^{-1}$]	-7.29		-7.21			-7.81		-6.89[a]			-7.50	

t.w.=this work; KH1997a=Koesterke and Hamann (1997a); KH1997b=Koesterke and Hamann (1997b); M2007=Marcolino et al. (2007b), BH1982=Barlow and Hummer (1982)

[a] Values obtained assuming $\log L/L_\odot$=3.84.

[b] Not constrained. Value assumed on the grid models was kept.

[c] Distances from Table 1.

Results

Table 5. Parameters of our best-fitting models for the sample objects and distance dependent parameters. X_{He}, X_C, X_N, X_O, and X_{Ne} are the helium, carbon, nitrogen, oxygen, and neon mass fractions, respectively. For the discussion on the derived parameters and errors, see text. Results by other authors are also shown.

Object	Pb 6		NGC 6905			NGC 5189		Sand 3			NGC 2867	
	t.w.	KH1997a	t.w.	M2007	KH1997a	t.w.	KH1997a	t.w.	KH1997b	BH1982	t.w.	KH1997a
T_* [kK]	165	140	150	149.6	141	165	135	150	140	200	165	141
R_t [$R_\odot$]	9.9	4.5	10.7	10.5	3.4	9.9	5.0	9.4	3.0		8.5	4.0
v_∞ [km/s]	2500	3000	2000	1890	1800	2500	3000	2200	2200	2700	2000	1800
X_{He}	0.49	0.617	0.45	0.49	0.60	0.58	0.757	0.28	0.615	0.38	0.60	0.66
X_C	0.35	0.24	0.45	0.40	0.25	0.25	0.16	0.55	0.26	0.54	0.25	0.25
X_O	0.12	0.14	0.08	0.10	0.15	0.12	0.08	0.08	0.12	0.08	0.10	0.09
X_N	0.03	0.003	0.00011	<0.001	0	0.01	0.003	0.07	0.005		0.01[b]	0
X_{Ne}	0.01		0.02			0.04		0.02[b]			0.04	
ξ_{max} [km/s]	200		150			200		150			200	
d[c][kpc]	4.38		1.70			0.55		0.80[a]			1.84	
distance dependent parameters												
R_* [$R_\odot$]	0.06		0.09			0.03		0.12[a]			0.05	
$\log L/L_\odot$	3.43		3.56			2.73		3.84[a]			3.15	
$log \dot{M}$ [$M_\odot yr^{-1}$]	-7.29		-7.21			-7.81		-6.89[a]			-7.50	

t.w.=this work; KH1997a=Koesterke and Hamann (1997a); KH1997b=Koesterke and Hamann (1997b); M2007=Marcolino et al. (2007b), BH1982=Barlow and Hummer (1982)

[a] Values obtained assuming $\log L/L_\odot$=3.84.

[b] Not constrained. Value assumed on the grid models was kept.

[c] Distances from Table 1.

Results

Table 5. Parameters of our best-fitting models for the sample objects and distance dependent parameters. X_{He}, X_C, X_N, X_O, and X_{Ne} are the helium, carbon, nitrogen, oxygen, and neon mass fractions, respectively. For the discussion on the derived parameters and errors, see text. Results by other authors are also shown.

Object	Pb 6		NGC 6905			NGC 5189		Sand 3			NGC 2867	
	t.w.	KH1997a	t.w.	M2007	KH1997a	t.w.	KH1997a	t.w.	KH1997b	BH1982	t.w.	KH1997a
T_* [kK]	165	140	150	149.6	141	165	135	150	140	200	165	141
R_t [$R_\odot$]	9.9	4.5	10.7	10.5	3.4	9.9	5.0	9.4	3.0		8.5	4.0
v_∞ [km/s]	2500	3000	2000	1890	1800	2500	3000	2200	2200	2700	2000	1800
X_{He}	0.49	0.617	0.45	0.49	0.60	0.58	0.757	0.28	0.615	0.38	0.60	0.66
X_C	0.35	0.24	0.45	0.40	0.25	0.25	0.16	0.55	0.26	0.54	0.25	0.25
X_O	0.12	0.14	0.08	0.10	0.15	0.12	0.08	0.08	0.12	0.08	0.10	0.09
X_N	0.03	0.003	0.00011	<0.001	0	0.01	0.003	0.07	0.005		0.01[b]	0
X_{Ne}	0.01		0.02			0.04		0.02[b]			0.04	
ξ_{max} [km/s]	200		150			200		150			200	
d[c][kpc]	4.38		1.70			0.55		0.80[a]			1.84	
distance dependent parameters												
R_* [$R_\odot$]	0.06		0.09			0.03		0.12[a]			0.05	
$\log L/L_\odot$	3.43		3.56			2.73		3.84[a]			3.15	
$log\dot{M}$ [$M_\odot yr^{-1}$]	-7.29		-7.21			-7.81		-6.89[a]			-7.50	

t.w.=this work; KH1997a=Koesterke and Hamann (1997a); KH1997b=Koesterke and Hamann (1997b); M2007=Marcolino et al. (2007b), BH1982=Barlow and Hummer (1982)

[a] Values obtained assuming $\log L/L_\odot$=3.84.

[b] Not constrained. Value assumed on the grid models was kept.

[c] Distances from Table 1.

Results

Table 5. Parameters of our best-fitting models for the sample objects and distance dependent parameters. X_{He}, X_C, X_N, X_O, and X_{Ne} are the helium, carbon, nitrogen, oxygen, and neon mass fractions, respectively. For the discussion on the derived parameters and errors, see text. Results by other authors are also shown.

Object	Pb 6		NGC 6905			NGC 5189		Sand 3			NGC 2867	
	t.w.	KH1997a	t.w.	M2007	KH1997a	t.w.	KH1997a	t.w.	KH1997b	BH1982	t.w.	KH1997a
T_* [kK]	165	140	150	149.6	141	165	135	150	140	200	165	141
R_t [R$_\odot$]	9.9	4.5	10.7	10.5	3.4	9.9	5.0	9.4	3.0		8.5	4.0
v_∞ [km/s]	2500	3000	2000	1890	1800	2500	3000	2200	2200	2700	2000	1800
X_{He}	0.49	0.617	0.45	0.49	0.60	0.58	0.757	0.28	0.615	0.38	0.60	0.66
X_C	0.35	0.24	0.45	0.40	0.25	0.25	0.16	0.55	0.26	0.54	0.25	0.25
X_O	0.12	0.14	0.08	0.10	0.15	0.12	0.08	0.08	0.12	0.08	0.10	0.09
X_N	0.03	0.003	0.00011	<0.001	0	0.01	0.003	0.07	0.005		0.01[b]	0
X_{Ne}	0.01		0.02			0.04		0.02[b]			0.04	
ξ_{max} [km/s]	200		150			200		150			200	
d[c][kpc]	4.38		1.70			0.55		0.80[a]			1.84	
distance dependent parameters												
R$_*$ [R$_\odot$]	0.06		0.09			0.03		0.12[a]			0.05	
log $L/L_\odot$	3.43		3.56			2.73		3.84[a]			3.15	
$log\dot{M}$ [M$_\odot$yr^{-1}]	-7.29		-7.21			-7.81		-6.89[a]			-7.50	

t.w.=this work; KH1997a=Koesterke and Hamann (1997a); KH1997b=Koesterke and Hamann (1997b); M2007=Marcolino et al. (2007b), BH1982=Barlow and Hummer (1982)

[a] Values obtained assuming log $L/L_\odot$=3.84.

[b] Not constrained. Value assumed on the grid models was kept.

[c] Distances from Table 1.

Results

Table 5. Parameters of our best-fitting models for the sample objects and distance dependent parameters. X_{He}, X_C, X_N, X_O, and X_{Ne} are the helium, carbon, nitrogen, oxygen, and neon mass fractions, respectively. For the discussion on the derived parameters and errors, see text. Results by other authors are also shown.

Object	Pb 6		NGC 6905			NGC 5189		Sand 3			NGC 2867	
	t.w.	KH1997a	t.w.	M2007	KH1997a	t.w.	KH1997a	t.w.	KH1997b	BH1982	t.w.	KH1997a
T_* [kK]	165	140	150	149.6	141	165	135	150	140	200	165	141
R_t [$R_\odot$]	9.9	4.5	10.7	10.5	3.4	9.9	5.0	9.4	3.0		8.5	4.0
v_∞ [km/s]	2500	3000	2000	1890	1800	2500	3000	2200	2200	2700	2000	1800
X_{He}	0.49	0.617	0.45	0.49	0.60	0.58	0.757	0.28	0.615	0.38	0.60	0.66
X_C	0.35	0.24	0.45	0.40	0.25	0.25	0.16	0.55	0.26	0.54	0.25	0.25
X_O	0.12	0.14	0.08	0.10	0.15	0.12	0.08	0.08	0.12	0.08	0.10	0.09
X_N	0.03	0.003	0.00011	<0.001	0	0.01	0.003	0.07	0.005		0.01[b]	0
X_{Ne}	0.01		0.02			0.04		0.02[b]			0.04	
ξ_{max} [km/s]	200		150			200		150			200	
d[c][kpc]	4.38		1.70			0.55		0.80[a]			1.84	
distance dependent parameters												
R_* [$R_\odot$]												
$\log L/L_\odot$												
$\log \dot{M}$ [$M_\odot yr^{-1}$]												

Koesterke and Hamann 1997a,b: 0.19< C:He <0.7 for **[WCE]** stars
Leuenhagen et al. 1996: C:He typically **higher than 1** for **[WCL]** stars
T.W.: C:He =**0.42, 0.43, 0.71, 1.0, 1.96**.

t.w.=this work; KH1997a=Koesterke and Hamann (1997a); KH1997b=Koesterke and Hamann (1997b); M2007=Marcolino et al. (2007b), BH1982=Barlow and Hummer (1982)

[a]Values obtained assuming $\log L/L_\odot$=3.84.

[b]Not constrained. Value assumed on the grid models was kept.

[c]Distances from Table 1.

Results

Table 5. Parameters of our best-fitting models for the sample objects and distance dependent parameters. X_{He}, X_C, X_N, X_O, and X_{Ne} are the helium, carbon, nitrogen, oxygen, and neon mass fractions, respectively. For the discussion on the derived parameters and errors, see text. Results by other authors are also shown.

Object	Pb 6		NGC 6905			NGC 5189		Sand 3			NGC 2867	
	t.w.	KH1997a	t.w.	M2007	KH1997a	t.w.	KH1997a	t.w.	KH1997b	BH1982	t.w.	KH1997a
T_* [kK]	165	140	150	149.6	141	165	135	150	140	200	165	141
R_t [$R_\odot$]	9.9	4.5	10.7	10.5	3.4	9.9	5.0	9.4	3.0		8.5	4.0
v_∞ [km/s]	2500	3000	2000	1890	1800	2500	3000	2200	2200	2700	2000	1800
X_{He}	0.49	0.617	0.45	0.49	0.60	0.58	0.757	0.28	0.615	0.38	0.60	0.66
X_C	0.35	0.24	0.45	0.40	0.25	0.25	0.16	0.55	0.26	0.54	0.25	0.25
X_O	0.12	0.14	0.08	0.10	0.15	0.12	0.08	0.08	0.12	0.08	0.10	0.09
X_N	0.03	0.003	0.00011	<0.001	0	0.01	0.003	0.07	0.005		0.01[b]	0
X_{Ne}	0.01		0.02			0.04		0.02[b]			0.04	
ξ_{max} [km/s]	200		150			200		150			200	
d[c][kpc]	4.38		1.70			0.55		0.80[a]			1.84	
distance dependent parameters												
R_* [$R_\odot$]	0.06		0.09			0.03		0.12[a]			0.05	
$\log L/L_\odot$	3.43		3.56			2.73		3.84[a]			3.15	
$\log \dot{M}$ [$M_\odot yr^{-1}$]	-7.29		-7.21			-7.81		-6.89[a]			-7.50	

t.w.=this work; KH1997a=Koesterke and Hamann (1997a); KH1997b=Koesterke and Hamann (1997b); M2007=Marcolino et al. (2007b), BH1982=Barlow and Hummer (1982)

[a]Values obtained assuming $\log L/L_\odot$=3.84.

[b]Not constrained. Value assumed on the grid models was kept.

[c]Distances from Table 1.

Results

Table 5. Parameters of our best-fitting models for the sample objects and distance dependent parameters. X_{He}, X_C, X_N, X_O, and X_{Ne} are the helium, carbon, nitrogen, oxygen, and neon mass fractions, respectively. For the discussion on the derived parameters and errors, see text. Results by other authors are also shown.

Object	Pb 6		NGC 6905			NGC 5189		Sand 3			NGC 2867	
	t.w.	KH1997a	t.w.	M2007	KH1997a	t.w.	KH1997a	t.w.	KH1997b	BH1982	t.w.	KH1997a
T_* [kK]	165	140	150	149.6	141	165	135	150	140	200	165	141
R_t [R$_\odot$]	9.9	4.5	10.7	10.5	3.4	9.9	5.0	9.4	3.0		8.5	4.0
v_∞ [km/s]	2500	3000	2000	1890	1800	2500	3000	2200	2200	2700	2000	1800
X_{He}	0.49	0.617	0.45	0.49	0.60	0.58	0.757	0.28	0.615	0.38	0.60	0.66
X_C	0.35	0.24	0.45	0.40	0.25	0.25	0.16	0.55	0.26	0.54	0.25	0.25
X_O	0.12	0.14	0.08	0.10	0.15	0.12	0.08	0.08	0.12	0.08	0.10	0.09
X_N	0.03	0.003	0.00011	$<$0.001	0	0.01	0.003	0.07	0.005		0.01[b]	0
X_{Ne}	0.01		0.02			0.04		0.02[b]			0.04	
ξ_{max} [km/s]	200		150			200		150			200	
d[c][kpc]	4.38		1.70			0.55		0.80[a]			1.84	
distance dependent parameters												
R$_*$ [R$_\odot$]	0.06		0.09			0.03		0.12[a]			0.05	
log $L/L_\odot$	3.43		3.56			2.73		3.84[a]			3.15	
$log \dot{M}$ [M$_\odot$yr^{-1}]	-7.29		-7.21			-7.81		-6.89[a]			-7.50	

t.w.=this work; KH1997a=Koesterke and Hamann (1997a); KH1997b=Koesterke and Hamann (1997b); M2007=Marcolino et al. (2007b), BH1982=Barlow and Hummer (1982)

[a] Values obtained assuming log $L/L_\odot$=3.84.

[b] Not constrained. Value assumed on the grid models was kept.

[c] Distances from Table 1.

This Work x Literature: Abundances

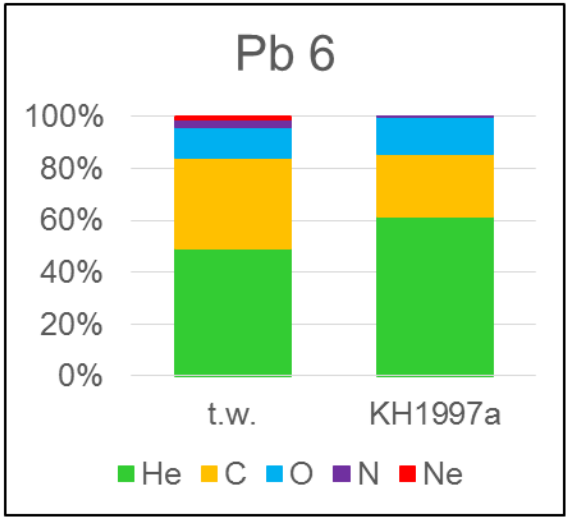

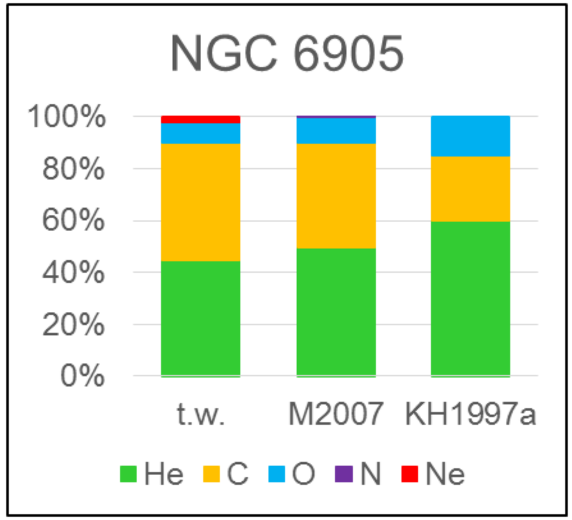

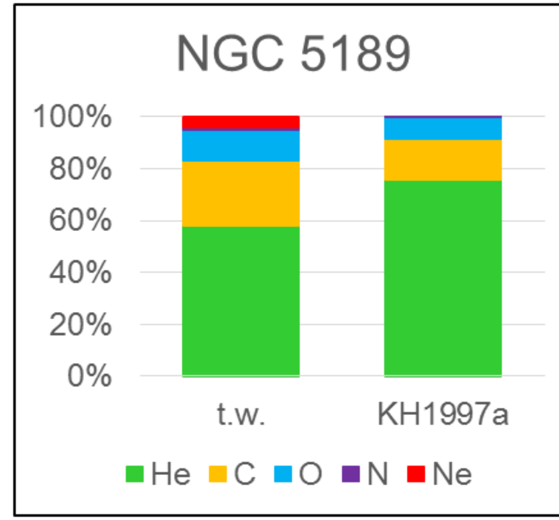

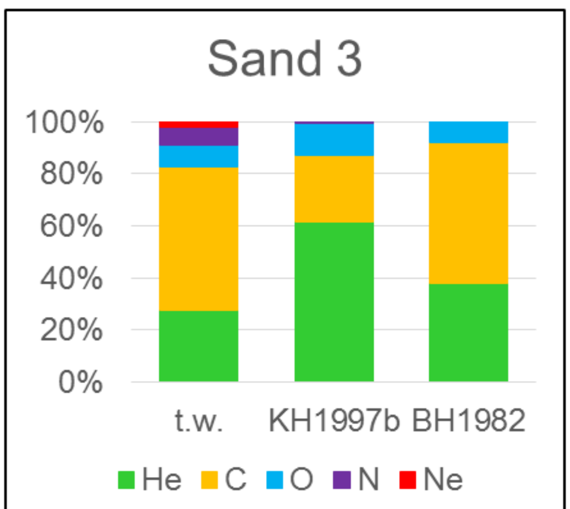

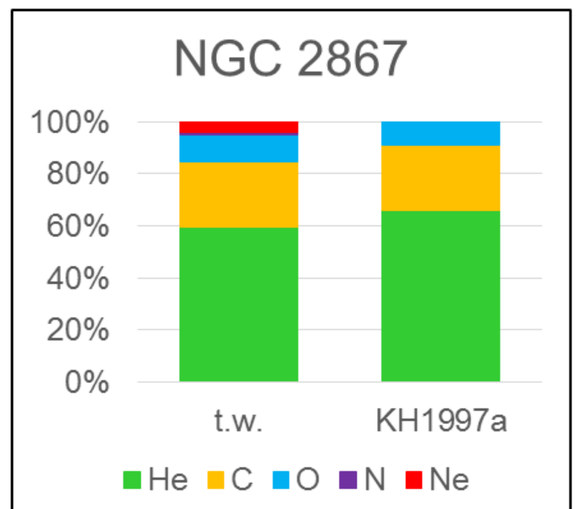

This Work x Literature: Abundances

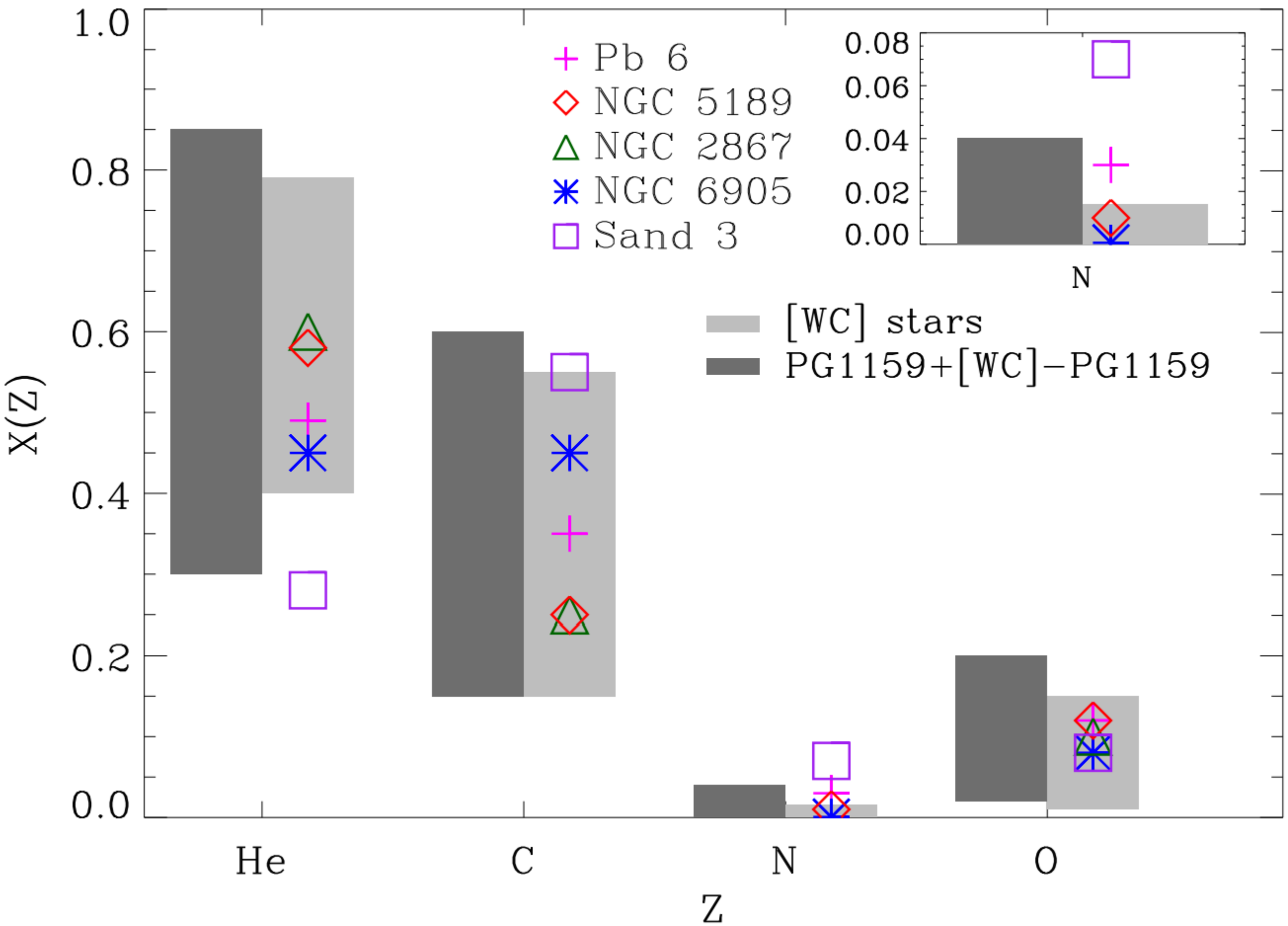

Figure 14. The abundance intervals of PG1159, [WC]-PG1159 and [WC] stars (as found from the literature) are compared to the values determined in this work.

Evolutionary Tracks

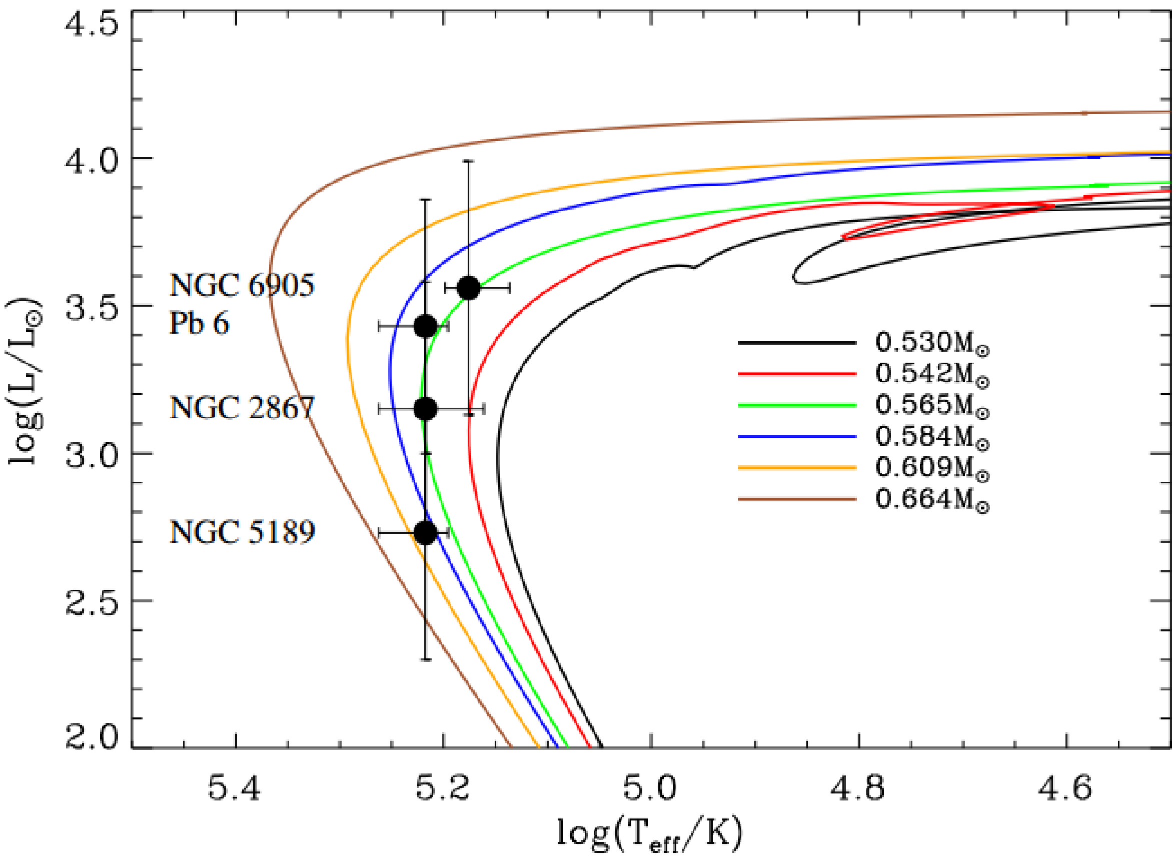

Figure 13. HR diagram with evolutionary tracks from Miller Bertolami and Althaus (2006). The open circles correspond to the sample objects. Sand 3 was omitted from it, because, to the best of our knowledge, there is no measurement of its distance in the literature.

Conclusions

Concluding…

◈We analyzed UV spectra from 5 of the hottest known [WCE]-type CSPNe using our grid of synthetic spectra, calculated with CMFGEN.

◈Grids available at

http://dolomiti.pha.jhu.edu/planetarynebulae.html
http://www.astro.iag.usp.br/~graziela/GRIDWEB/front.html

◈We found line blanketing of Ni, Co, Mg, and Na to improve the fit of the OV lines in all objects analyzed.

◈We revised up the temperatures for NGC 5189, NGC2867 and Pb 6.

◈We revised up the values of N abundances.

◈We constrained Ne mass fractions for the first time in [WCE] stars.

◈C:He mass ratios found by us span a wide range of values: 0.42 < C:He < 1.96 .

References:

Herwig F., 2005, ARA&A, 43, 435

Hillier, D.J., Miller, D.L., 1998, ApJ, 496, 407

Keller, G. R., Herald, J. E., Bianchi L., Maciel, W. J., Bohlin R. C., 2011, MNRAS, 705

Koesterke, L., Dreizler, S., Rauch, T., 1998, A&A, 330, 1041

Miller Bertolami, M. M., Althaus, L. G., 2006, A&A, 454, 845

Stanghellini, L., R. A. Shaw, E. Villaver, 2008, ApJ, 689,194

Werner, K., Rauch, T., Kruk, J.W., 2010, ApJL, 719, L32

Werner, K., Rauch, T., Kruk, J.W., Kurucz, R.L., 2011, A&A, 531, A146

Acknowledgements:

CAPES-0370-09-6, Fapesp-06/58240-3 and 2012/03479-2 grants.

The data presented were obtained from MAST.